

~~7-7-0083~~

**CASE FILE  
COPY**

Heat Transfer  
Laboratory[illegible]



THERMAL CONTACT RESISTANCE WITH  
NON-UNIFORM INTERFACE PRESSURES

R. McMillan, Jr.  
B.B. Mikic'

Prepared for the National Aeronautics  
and Space Administration  
Grant No. NGR-22-009-(477)

November 1970

DSR PROJECT 72105

Engineering Projects Laboratory  
Department of Mechanical Engineering  
Massachusetts Institute of Technology  
Cambridge, Massachusetts 02139

# ABSTRACT

This work considers the effect of roughness and waviness on interfacial pressure distributions and interfacial contact resistance. It is shown that for moderate roughness the contour area could be substantially different from the contour area calculated using the Hertzian theory. The model for pressure calculation assumes plastic deformation of surface irregularities and elastic deformation of a spherically wavy base. The calculations of pressure distributions cover the range of parameters of practical interest. Experimental contact resistance values have been determined and are compared with theoretical predictions. It was calculated that contact conductance for wavy surfaces can be increased for certain ranges of parameters by making surfaces rough.

#### ACKNOWLEDGMENTS

This report was supported by the National Aeronautics and Space Administration under Grant No. NGR-22-009-(477).

TABLE OF CONTENTS

	Page
ABSTRACT . . . . .	2
ACKNOWLEDGMENTS . . . . .	3
TABLE OF CONTENTS . . . . .	4
LIST OF FIGURES . . . . .	6
NOMENCLATURE . . . . .	7
1. INTRODUCTION . . . . .	10
2. DESCRIPTION OF SURFACES . . . . .	14
3. INTERFACE PRESSURE DISTRIBUTION . . . . .	15
3.1 Governing Equations	15
3.2 Method of Solution	16
3.3 Pressure Distribution Curves	17
4. EXPERIMENTAL PROGRAM . . . . .	19
4.1 Preparation of Specimens	19
4.2 Description of the Apparatus	20
4.3 Experimental Procedure	22
5. EXPERIMENTAL RESULTS AND DISCUSSIONS . . . . .	23
6. CONCLUSIONS . . . . .	24
BIBLIOGRAPHY . . . . .	25
APPENDIX A - DERIVATION OF CONTACT RESISTANCE EQUATION . . . . .	27
APPENDIX B - COMPUTER PROGRAMS . . . . .	30
List of Fortran Variables Used in Programs	30
Program to Determine Dimensionless Pressure Distributions Between Rough and Wavy Surfaces	32
Program to Determine Contact Resistance Using Equation (5)	40

	Page
APPENDIX C - TABLES OF COORDINATES FOR PRESSURE DISTRIBUTIONS .	46
TABLE I - EXPERIMENTAL DATA . . . . .	71
TABLE II - EXPERIMENTAL DATA . . . . .	72
FIGURES . . . . .	73

LIST OF FIGURES

Fig. 1	Definition of Contact Resistance
Fig. 2	Surface Contacts
Fig. 3	Surface Waviness
Fig. 4	Surface Geometry
Fig. 5	Typical Contact Area
Fig. 6	Plasticity Index vs. Dimensionless Force: Region of Significance for Roughness
Fig. 7 - 16	Dimensionless Pressure Distribution Curves
Fig. 17 - 19	Comparison of Hertzian and Rough-Sphere Pressure Distributions
Fig. 20	Radius Ratios: Smooth vs. Rough Spheres
Fig. 21	Surface-Profile Measuring Device
Fig. 22	Contact Resistance Apparatus
Fig. 23	Contact Conductance Results
Fig. 24	Non-Uniform Heat Transfer Coefficient
Fig. 25	Non-Uniform Heat Transfer Coefficient



# NOMENCLATURE

$a_H$	Hertzian radius
$\bar{a}_H$	Dimensionless Hertzian radius, $a_H/(R_1\sigma)^{1/2}$
$a_w$	Contour radius
$A$	Area
$A_{app}$	Apparent contact area
$A_c$	Contour area
$\bar{A}$	$A/R_1\sigma$
$b$	Radius of heat channel
C.L.A.	Centerline average
$C_n$	Constant inside a summation
$E_1, E_2$	Moduli of elasticity of specimens in contact
$\bar{E}$	$\equiv \left( \frac{1 - \nu_1^2}{\pi E_1} + \frac{1 - \nu_2^2}{\pi E_2} \right)^{-1}$
$F$	Force
$\bar{F}$	$F/H\sigma R_1$
$f(\lambda)$	$h/h_{av}$
$H$	Microhardness of the softer of two materials in contact
$h$	Wave amplitude; Heat transfer coefficient
$h_{av}$	Average heat transfer coefficient
$J_n$	Bessel function of order $n$
$k$	Thermal conductivity--if two materials are in contact, $k = 2k_1k_2/(k_1 + k_2)$
$P$	Pressure
$P_{av}$	Average pressure

$P_a$	Average pressure over contour area
$P_H$	Hertzian pressure
$P_L$	Local pressure over Hertzian area
$\overline{P}$	$P/H$
$Pl$	Plasticity index $\equiv (\overline{E}/H) (\sigma/R_1)^{1/2}$
$Q$	Heat
$q/A, Q/A$	Heat flux over surface A
$R$	Thermal resistance; Radius of curvature
$R_c$	Constriction resistance
$R_1$	$R_1 R_2 / (R_1 + R_2)$
$R_1, R_2$	Radii of curvature of undeformed, spherically wavy surfaces
$R_{MAC}$	Macroscopic resistance term
$r$	Radial coordinate parallel to contact interface plane
$\overline{r}$	$r / (R_1 \sigma)^{1/2}$
$r_1$	A quarter-wavelength
$r_o$	Radius where pressure becomes zero
$T_c$	Local surface temperature
$T_o$	Ambient temperature
$T_s$	Extrapolated surface temperature
$w(r)$	Deformation of spherical object at point r
$Y$	Distance between the mean lines of specimen surfaces, measured in a direction perpendicular to the interface plane
$\overline{Y}$	$Y/\sigma$
$y_1$	Slope of a surface profile at position 1

**z**                      Vertical distance coordinate

Greek Letter Symbols

$\lambda$                       r/b

$\nu_n$                       Roots of  $J_1(\nu_n) = 0$

$\nu_1, \nu_2$                       Poisson's ratio of specimens in contact

$\rho$                       Distance between any point r and any elemental area  
dA on the interfacial area

$\bar{\rho}$                        $(\rho)/(R_1\sigma)^{1/2}$

$\sigma$                       Root mean square deviation of roughness heights--  
 $\sigma = (\sigma_1^2 + \sigma_2^2)^{0.5}$  when two surfaces are in contact

$\text{Tan}\theta$                       Mean absolute value of profile slopes-- $\text{Tan}\theta = (\text{Tan}_1^2\theta + \text{Tan}_2^2\theta)^{0.5}$   
if two surfaces are in contact. More specifically,  
 $\text{Tan}\theta_i \equiv \lim_{L \rightarrow \infty} \frac{1}{L} \int_0^L |y_1'| dx; \quad i = 1, 2, \dots$

$\phi_w$                       Contact resistance factor

## 1. INTRODUCTION

Thermal resistances discussed in this work are assumed to occur in a vacuum environment, or in an environment where an interstitial fluid has a very low thermal conductivity. Thermal contact resistance is defined by

$$R = \frac{\Delta T}{q/A} \quad (1)$$

where  $(q/A)$  is the heat flux based on the apparent area, and  $\Delta T$  is defined in Figure 1. Consider two pieces of smooth metal that are pressed together. As seen in Figure 2A, there is a finite number of contact points,  $A_c$ . The total actual contact area is often much smaller than the apparent area,  $A_{app}$ . Resistance to heat flow across such a joint is called contact resistance due to macroscopic constriction. The term "constriction" is used because heat-flow lines must squeeze together to pass through the contact area (see Figure 2B). Of course, the constriction would be present only in a vacuum, or where the interstitial fluid has a lower conductivity than the base material. If the surfaces are rough (Figure 2C), the true contact area will be even smaller than  $A_c$ . For this reason,  $A_c$  will from now on be referred to as a "contour area" rather than a "contact area." The additional area reduction due to roughness causes "microscopic constriction" of the heat-flow lines.

If  $A_c = A_{app}$ , only microscopic constriction is present, and the pressure distribution over the contour area is uniform. When both macroscopic and microscopic constriction are present, the pressure distribution is non-uniform, because of the clustering of contour areas at discrete locations.

Holm [6], Kragelski [7], Clausing [1], and Greenwood [3] developed equations for contact resistance under these conditions. They superimposed a microscopic constriction relation over another equation that applies to the macroscopic case. These relations, however, require a detailed knowledge of the contour area. Consider heat flow between two cylindrical solids whose channel radii are greater than the radius of their contour area (as in Figure 2B). In addition, let the surfaces originally be spherically wavy. There are three ways that one can model the heat transfer across the interface:

1. Assume constant temperature across the contour area;
2. Assume constant flux across the contour area; or
3. Assume that the heat flux through any point on the contour area is proportional to the microscopic conductance, which is in turn a function of the local pressure between the two surfaces.

In the first case, the maximum heat flux occurs at the outer rim of the contour area. For this reason, heat-flow lines that are outside the contour radius as  $Z \rightarrow \infty$  must change their direction a minimal amount. The third case, however, places the maximum heat flux at the center of the contour area, making it necessary for the outer heat-flow lines to change direction substantially more. In the second case above, heat-flow is distributed in some intermediate fashion.

Resistance to heat flow is highest when the heat-flow lines must redistribute themselves to the greatest extent. For this reason, a contact resistance formula employing assumption (3) will be an upper bound for the actual contact resistance. Case (1) will consequently be a lower bound, and case (2) will fall somewhere in the middle.

A simple formula, e.g., Reference [2], predicts the macroscopic constriction resistance from the radius of the contour area:

$$R_{MAC} = \frac{\phi_w \pi b^2}{2k a_w} \quad (2)$$

where  $a_w$  is the contour radius,  $b$  is the channel radius, and  $k$  is the thermal conductivity.  $\phi_w$ , the contact resistance factor, is given by

$$\phi = \left(1 - \frac{a_w}{b}\right)^{1.5}$$

where constant temperature is assumed and by

$$\phi = \frac{32}{3\pi^2} \left(1 - \frac{a_w}{b}\right)^{1.5}$$

for the case of constant flux. A similar resistance equation includes the effect of microscopic constriction resistance [9]:

$$R = \frac{b^2}{a_w^2} \frac{1}{h_c} + \frac{\phi_w \pi b^2}{2k a_w} \quad (3)$$

where

$$h_c = 1.45 \left(\frac{P_a}{H}\right)^{0.985} \frac{k \tan\theta}{\sigma} \quad (4)$$

$\tan\theta$  is the mean absolute value of the profile slopes, and  $\sigma$  is the root-mean square deviation of roughness heights.  $P_a$  is the average pressure over the contour area,  $\pi a_w^2$ .

We now have equations for models (1) and (2), assuming constant temperature or constant heat-flux across the contour area. Mikic [8] has developed an equation that falls into the third category, where contact resistance is a function of the contour area pressure distribution,  $P(r)$ :

$$R = 0.345 \frac{\sigma}{k \tan \theta} \left[ \int_0^1 \lambda \left( \frac{P}{H} \right)^{0.985} d\lambda \right]^{-1} + \frac{8b}{k} \sum_{n=1}^{\infty} \frac{\left[ \int_0^1 \lambda \left( \frac{P}{P_{av}} \right)^{0.985} J_0(v_n \lambda) d\lambda \right]^2}{v_n J_0^2(v_n)} \quad (5)$$

$b$ ,  $\sigma$ , and  $\tan \theta$  have been defined above. Hardness and thermal conductivity are denoted by  $H$  and  $k$ , respectively, and  $\lambda$  is the dimensionless radial coordinate  $\lambda \equiv r/b$ .  $J_n$  is the Bessel function of order  $n$ , and  $v_n$  are the roots of

$$J_1(v_n) = 0.$$

$P_{av}$  is the average pressure over the apparent area. A summary of the derivation of this equation appears in Appendix A. Knowledge of the interfacial pressure distribution is required for this equation. The Hertzian pressure distribution for a smooth sphere pressed against a rigid flat plane cannot, in general, be used as an approximation. Greenwood [4] has shown that in many instances the pressure distribution under a rough sphere is substantially different from the Hertzian approximation.

This work evaluates numerically the required pressure distribution curves for rough, wavy surfaces in contact. The curves are compiled in terms of convenient dimensionless parameters. In addition, experimental values of contact resistance are presented and compared with theoretical results.

The model used in this work assumes that microscopic surface irregularities are random and normally distributed, and their deformation is plastic. Deformation of the spherically wavy base surface is elastic.

## 2. DESCRIPTION OF SURFACES

The surfaces considered in this investigation are both wavy and rough. A surface is wavy if its profile has a finite radius of curvature along some finite length (see Figure 3). Roughness appears as a zig-zag pattern of surface heights superimposed over the waviness. The surfaces considered are assumed to have a Gaussian distribution of heights. It has been shown in Reference [2] that for the purpose of determining contact resistance, the parameters  $\sigma$ ,  $\tan\theta$ , and  $R$  provide a sufficient description of the surfaces involved.  $\sigma$  is the root-mean-square deviation of roughness heights, and  $\tan\theta$  is the absolute slope of these irregularities. In a wavy surface,  $R$  is the radius of curvature of a half-wave. A convenient way of finding  $R$  is by charting the surface profile and using the following equation (refer to Figure 3):

$$R = \frac{(\frac{1}{4} \text{ wavelength})^2}{2 (\text{wave amplitude})} = \frac{r_1^2}{2h} \quad , \quad (\text{for } \frac{h}{R} \ll 1) \quad . \quad (6)$$

A description of surface-profile measuring devices is given later on in this paper.



### 3. INTERFACE PRESSURE DISTRIBUTION

#### 3.1 Governing Equations

The following equations determine the pressure distribution between two rough and wavy surfaces in contact under a load F:

$$P = \frac{H}{2} \text{ERFC} \left( \frac{Y}{\sqrt{2} \sigma} \right) \quad (7)$$

$$Y(r) = Y(0) + \frac{r^2 (R_1 + R_2)}{2 R_1 R_2} - \frac{2\pi}{E} \int P \, dr + \frac{1}{E} \iint_A \frac{P}{\rho} \, dA \quad (8)$$

$$F = \iint_A P \, dA . \quad (9)$$

Non-dimensional versions of these equations are:

$$\bar{P} = \frac{1}{2} \text{ERFC} \left( \frac{\bar{Y}}{\sqrt{2}} \right) \quad (7a)$$

$$\bar{Y}(F) = \bar{Y}(0) + \frac{1}{2} \bar{r}^2 - \frac{2\pi}{P\ell} \int \bar{P} \, d\bar{r} + \frac{1}{P\ell} \iint_{\bar{A}} \frac{\bar{P}}{\bar{\rho}} \, d\bar{A} \quad (8a)$$

$$\bar{F} = \iint_{\bar{A}} \bar{P} \, d\bar{A} . \quad (9a)$$

The variables in these equations are defined in the Nomenclature and Figures 4A, 4B, and 5.

Equations (7) and (7A) come from surface-height distribution theory and the assumption of plastic deformation of surface asperities [2]. Equations (8) and (8A) result from geometry and an assumed elastic deformation [11] as seen in Figure 4A. The final equation is a simple force balance which must be satisfied. The solution of these equations is described in Section 3.2.

The non-dimensional version of these equations results in (dimensionless) pressure vs. (dimensionless) radius curves that are functions of only two parameters,  $P_1$  and  $\bar{F}$ . For practical purposes, the most useful plasticity index values range from 0.0 to 0.6. These values correspond to metals such as copper, aluminum, and stainless steel, with root-mean-square roughnesses from 20 micro-inches to 200 micro-inches, and whose wavy surfaces have radii of curvature between 25 inches to infinity.

### 3.2 Method of Solution

This section describes the technique used to find a pressure distribution employed by the contact resistance equation (Equation (5)). A pressure distribution is determined by an iterative procedure that refines a rough approximation until all three of the governing equations (7), (8), and (9) are simultaneously satisfied.

The Hertz solution for a smooth sphere pressed against a rigid flat wall [11] is taken as a first approximation for  $Y(r)$ . This  $Y(r)$  is substituted into Equation (7) whose pressure is in turn placed in Equation (8) along with an arbitrary constant value of  $Y(0)$ . The new  $Y(r)$  found from Equation (8) is then placed in Equation (7) and checked by (9) to determine if its load matches the actual load. At this point,  $Y(0)$  is repeatedly modified until the pressures in (9) yield a force that is within 10 per cent of the correct load.

In some cases the calculated load will be lower than the actual load even when  $Y(0) = 0$ . Thus it would be impossible to reach the correct load by merely modifying  $Y(0)$ . When this condition exists,  $Y(0)$  is immediately called zero, and the resultant pressures are sent directly to Equation (8).

Here the shape of the pressure distribution is changed until the correct load can be obtained. When the iteration process passes through Equations (7) and (8) twice in a row yielding approximately the same pressures (within 1 per cent), the computation is complete, and the desired pressure distribution is printed.

Computations were made using an I.B.M. 360. For the cases presented in this work, twenty-four radial increments have been used in the finite difference approximations. To be sure that twenty-four increments were sufficient, a test case was run at forty-eight increments also. Comparison of the two resulting pressure curves shows a maximum discrepancy of 5 per cent and an average discrepancy of less than 1 per cent. Based on the above, it was concluded that twenty-four increments yield sufficient accuracy.

In the calculation procedure, symmetry was imposed on the bulk elastic deflection by setting  $w(0) = w(\Delta r)$  where  $w(0)$  is the deflection at the center and  $w(\Delta r)$  is the deflection at the first radial point. In this way, the slope of the deflection curve at the center line will be zero.

### 3.3 Pressure Distribution Curves

The Hertzian pressure distribution between two spherically wavy surfaces is given by

$$\bar{P} = \frac{1.5 \bar{F}}{\pi \bar{a}_H^2} (1 - (\bar{r}/\bar{a}_H)^2)^{0.5} \quad (10)$$

where  $\bar{F}$  is the dimensionless applied load, and  $\bar{a}_H$  is the dimensionless Hertzian radius,  $\bar{a}_H \equiv 1.333 (\bar{F}/P_1)^{1/3}$ .

When a surface is rough, the pressure distribution may or may not differ significantly from the Hertzian solution. The region of  $P_1$  vs.  $\bar{F}$

plane where roughness is significant has been determined in this work and is presented in Figure 6. Roughness causes pressure distributions to differ significantly from Hertzian predictions in the following regions:

$$\bar{F} < 12.8 (P1)^{1.25}, 0 < P1 < .10 \quad (11)$$

$$\bar{F} < 11.7 (P1) - 0.25, .10 < P1 < .60 \quad (12)$$

Even outside of these regions, edge effects will cause the contour radius to be greater than the Hertzian radius.

Dimensionless pressure curves for the region defined above appear in Figures 7-16. Coordinates for these and other pressure curves are listed in Appendix C. Pressure curves close to the transition line in Figure 6 closely resemble Hertzian shapes, whereas far below this line, curves are much flatter. Figures 17-19 illustrate this by depicting pressure curves at extreme values of  $\bar{F}$  along with the associated Hertzian pressures. In each of these pictures, the curve with the higher maximum is the Hertzian pressure ( $p_H$ ).

Let  $r_o$  be defined as the radial position where the pressure drops to zero.  $r_o$  is therefore the contour radius and is available from the enclosed pressure distribution solutions. The ratio of  $r_o$  over the Hertzian radius ( $a_H$ ) becomes less as the applied load is increased.  $r_o/a_H$  is plotted as a function of  $P1$  and  $\bar{F}$  in Figure 20.  $r_o/a_H$  approaches a constant value greater than one as  $\bar{F}$  values leave the region described by Equations (11) and (12). Outside this region,  $r_o$  should probably be used instead of  $a_H$  as the contour radius in Equations (2) and (3), whereas the Hertzian pressure distribution is in this case acceptable for Equation (5).

The  $r_o/a_H$  curves in Figure 20 are obtained from values of  $r_o$  which are read directly from Figures 8-16. There is some subjective interpretation as to where the pressure actually reaches zero. The behavior of the  $P_1 = .1$  curve should be accepted with caution because (as seen in Figure 8) only three  $r_o$  values were used to construct that curve.



#### 4. EXPERIMENTAL PROGRAM

##### 4.1 Preparation of Specimens

Experiments are performed with solid circular cylinders 1-1/2 inches long and 1 inch in diameter. The specimens are cut from stainless steel 303 bar-stock. Four holes (size 55 drill) are drilled to the centerline of each specimen so that thermocouples can be inserted for measurement of the axial temperature drop. The first hole is 1/4 inch from the interface, and the rest of the holes are 3/8 inch apart.

The contact resistance interface surfaces are lapped nominally flat. Waviness is created by the following method: A specimen is rotated in a lathe while a hard rubber block is used to press an abrasive (emery paper or diamond paste) against the test surface. The velocity distribution of the abrasive relative to the interface surface causes wear to be an increasing function of radius. In this way, the longer the abrasive is held in contact, the more convex the specimen becomes.

After the degree of waviness has been measured by a surface profilometer, the surface is blasted with glass beads to provide a desired roughness.

Waviness measurements are taken using a device specially built to accommodate the 1-inch diameter, 1-1/2-inch long specimens used in contact resistance experiments (see Figure 21). This device consists of a specimen holder that slides slowly beneath a diamond stylus that is connected to the core of a linear variable differential transformer. As the specimen passes underneath the stylus, the stylus moves up and down to follow the specimen surface. The profile shape is traced out on a Sanborn 150 recorder. This profilometer is capable of magnifying the vertical

deflection by a factor of five hundred. A detailed description of this device may be found in Reference [5].

Roughness is measured on a Taylor-Hobson Talysurf IV. The "Talysurf" provides a profile chart and a direct reading of the centerline average (C.L.A.). The root-mean-square roughness ( $\sigma$ ) can be determined by the following relation:

$$\sigma = [\text{C.L.A.}] (\pi/2)^{0.5} \approx 1.25 [\text{C.L.A.}] \quad (13)$$

The absolute value of the slope,  $\tan\theta$  can be computed graphically from the profile chart.

#### 4.2 Description of the Apparatus

Contact resistance data have been obtained from the apparatus in Figure 22. In a few words, the apparatus passes heat through two specimens in a vacuum environment. The three main sections of the apparatus are:

1. a vacuum chamber;
2. a refrigeration unit; and
3. a lever arrangement for applying an adjustable force to the test interface.

The vacuum system is basically a hollow aluminum cylinder which has been fabricated from four main sections. An upper cylinder is welded to a top plate. When the rig is in use, a removable lower cylinder with a flange seals up against an "O" ring and a bottom plate. The bottom plate is bolted to the supporting structure. The upper and lower cylinders are bolted together at their interface where another "O" ring allows for a vacuum seal. Connections with the vacuum pumps and the refrigeration unit are made through the bottom plate. Thermocouple wires, power lines



for the specimen heater, and a bellows for the loading mechanism enter through the top plate.

The vacuum is created by a forepump (Cenco HYVAC 14 rotary mechanical pump) and a 4-inch diameter diffusion pump (NRC model H4SP). A three-way valve allows the forepump to bring the system pressure down to 50 microns of mercury where activation of the diffusion pump will continue to lower the pressure to 15 microns of mercury.

The refrigeration unit, of course, supplies the low temperature sink for the heat fluxes that are passed through the test specimens. The unit is a 1-1/2 horsepower, Model 155 WFC, built by the Copeland Corporation. With its evaporator at 25 °F, it can receive up to 16,840 BTU/HR. Freon 12 serves as the refrigerant fluid. The magnitude of the heat-flux produced is crucial to contact resistance studies because with large loads too low a heat-flux will produce a negligible  $\Delta T$  across the test interface.

A series of levers, supported by a welded steel frame, permits the application of force to the specimens at a ratio of 100 to 1. This dead-weight loading is transmitted into the vacuum system via a 15-convolution, 3-3/8-inch I.D. stainless steel bellows, manufactured by the Flexonics Division of the Universal Oil Products Company. At atmospheric pressure, the applied load can be adjusted between 0 and 20,000 pounds. When the system is evacuated, the minimum load is 163 pounds, due to the atmosphere pressing down on the 3-3/8-inch diameter bellows device.

In addition to the apparatus listed above, there is a water-flow cooler between the bellows and the heater. This cooler prevents the heater from raising the temperature of the rest of the chamber to a level

that would destroy the vacuum seals. The heater is powered by a 220 volt d.c. power source. A more detailed description of this apparatus may be found in Reference [12].

#### 4.3 Experimental Procedure

Chromel-alumel thermocouples are covered with "Silver Goop" and inserted into the specimens. ("Silver Goop," manufactured by the Crawford Fitting Company, is a substance that provides a good thermal contact.) The thermocouple wires are then sealed in position with "White Epoxy," a product of the Hysol Division of the Dexter Corporation.

With the specimens inside, the vacuum chamber is sealed. The mechanical pump is switched on, and the system pressure is brought down to 50 microns of mercury. At this point the diffusion pump is activated to further lower the pressure to 15 microns of mercury. The applied load is now the minimum force of 163 pounds. After the water-flow cooler and the refrigeration unit are turned on, the heater is powered up to pass a heat-flux through the specimens.

Temperature readings are recorded from a thermocouple potentiometer every thirty minutes. When two successive readings are the same, it is assumed that steady state has been reached. The applied load is now increased, and the temperature-recording procedure is repeated. The applied load is always increased rather than decreased because the specimens may undergo a plastic (irreversible) deformation.

## 5. EXPERIMENTAL RESULTS AND DISCUSSION

The results of contact resistance experiments appear in Tables I and II and are plotted in Figures 23A and 23B. Also appearing are the predictions using Equation (2) for contact resistance with wavy surfaces, Equation (3) which includes the effects of both roughness and waviness, and Equation (5), an integral formula which assumes that the local interfacial flux is proportional to the local microscopic conductance and hence is a function of the local interfacial pressure. Equation (5) was solved on an I.B.M. 360 computer, using forty-four and eighty-nine radial increments (for the two different cases involved in the experiments) in a finite difference approximation of the integrals. The summation appearing in the macroscopic resistance term was evaluated using the first six terms of the series. The computer program for this equation appears in Appendix A. Equations (2) and (3) are given for the case of constant flux over the contour area, using two separate choices for the contour radius,  $a_w$ .

- a.  $a_w = a_H$ , the Hertzian (smooth surface) approximation; and
- b.  $a_w = r_o$ , the rough-surface contour radius determined from the pressure curves in Figures 7-16.

It has been stated earlier that Equation (5) is an upper bound for resistance (a lower bound for conductance). This indeed appears to be the case, as Equation (5) is the lowest curve in both Figures 23A and 23B. Using  $a_w = a_H$ , Equation (3) is very close to Equation (5). For the particular parameters involved in the experiments (for which the macroscopic conductance was the dominant factor), Equation (3) with  $a_w = r_o$

gives the best prediction for the actual contact conductance (to within 25 per cent accuracy).

It is important to notice that in certain ranges of parameters, a wavy surface will yield a higher  $h$  if it is roughened. This is caused, as it is shown in this work, by an increase in the contour area. (The engagement of the two surfaces covers a larger area when roughness is present as in Figure 4B.) Experimentally, this was also observed by Clausing [1]. He, however, did not explain the phenomena.

Experiments performed in this work dealt with surfaces that were both rough and wavy. There was no need to experiment with rough, flat surfaces, because this topic has already been covered sufficiently, both experimentally and theoretically, in Reference [2], for example. Similarly, the case of smooth, wavy surfaces has been covered amply by authors such as Clausing [1].

## 6. CONCLUSIONS

From pressure distribution curves given in Figures 7-16, one can determine the actual contour area between two rough and wavy surfaces. In a certain range of parameters, this contour area is substantially larger than the value calculated from the Hertzian theory. Experiments were performed in this range, and three basic approaches for the calculation of contact conductance were applied to the results, including formulas based on

- a. the Hertzian contour area;
- b. the contour area predicted by this work; and
- c. an integral relation which uses the complete interfacial pressure distribution.

It is suggested that Equation (3) (which assumes constant flux over the the contour area) using contour radii predicted in this work is the best prediction for the cases involved in the experiments (in which the predominant resistance comes from macroscopic constriction). For those cases where microscopic resistance is primarily controlling the value of contact resistance, it is believed that the integral relation (Equation (5)) would yield the correct prediction. (For the case of a uniform pressure distribution between two flat, rough surfaces, Equation (5) reduces to one term, the microscopic constriction resistance.)

The main conclusion is that contact conductance can be increased for certain ranges of parameters by making surfaces rough. This thesis also identifies the range of parameters where roughness will substantially affect the interfacial pressure distribution between rough and wavy surfaces.



BIBLIOGRAPHY

1. Clausing, A. M. and Chao, B. T., "Thermal Contact Resistance in a Vacuum Environment," National Aeronautics and Space Administration, University of Illinois, ME-TN-242-1, August, 1965.
2. Cooper, M., Mikic, B. B., and Yovanovich, M. M., "Thermal Contact Conductance," International Journal of Heat and Mass Transfer, V. 12, 1969, pp. 279-300.
3. Greenwood, J. A., "Constriction Resistance and the Real Area in Contact," British Journal of Applied Physics, 17, 1966, pp. 1621-1632.
4. Greenwood, J. A., "The Area of Contact between a Rough Surface and a Plane," Burndy Research Report No. 25, Burndy Corporation, Norwalk, Connecticut, July 30, 1965.
5. Henry, J. J., "Thermal Resistance of Metals in Contact," M.I.T. S. M. Thesis, August, 1961.
6. Holm, R., Electric Contact Handbook, Springer Verlag, Berlin, 1958.
7. Kragelski, I. and Demkin, M., "Contact Area of Rough Surfaces," Wear, V. 3, 1966, pp. 170-187.
8. Mikic, B. B., "Thermal Constriction Resistance Due to Non-Uniform Surface Conditions; Contact Resistance at Non-Uniform Interface Pressure." (This article, written under contract with the National Aeronautics and Space Administration, has been accepted for publication in the International Journal of Heat and Mass Transfer.)
9. Mikic, B. B. and Flengas, S., "Thermal Contact Resistance in a Vacuum under Conditions of Non-Uniform Interface Pressure." M.I.T. Heat Transfer Laboratory Memorandum, 1967.

10. Mikic, B. B. and Rohsenow, W. M., "Thermal Contact Resistance," M.I.T. Report No. DSR 74542-41, September, 1966.
11. Timoshenko, S. and Goodier, J. N., Theory of Elasticity, New York, McGraw-Hill, 1951.
12. Velissaropoulos, P. D., "Apparatus for Measurement of Contact Resistance," M.I.T. S. M. Thesis, August, 1963.
13. Yovanovich, M. M., "Thermal Contact Conductance in a Vacuum," M.I.T. Report No. DSR 4542-39, November, 1965.
14. Yovanovich, M. M. and Rohsenow, W. M., "Influence of Surface Roughness upon Thermal Contact Resistance," M.I.T. Report No. 76361-48, June, 1967.



## APPENDIX A

### DERIVATION OF CONTACT RESISTANCE EQUATION

The equation developed by Mikic [8] for contact resistance (Equation 5) was derived as follows:

Figure 24A depicts a solid circular cylinder with a non-uniform heat transfer coefficient,  $h$ , on the  $z = 0$  face. The sides are insulated, and heat-flow is assumed to be one-dimensional as  $z \rightarrow \infty$ . The flow of heat at the top surface is

$$Q = \int_A h (T_o - T_c) dA \quad (A1)$$

where  $T_o$  and  $T_c$  are defined in Figure 24A. The heat-flux over that surface is therefore

$$Q/A = T_o h_{av} - \frac{1}{A} \int_A T_c h dA \quad (A2)$$

where

$$h_{av} \equiv \frac{1}{A} \int_A h dA$$

The total resistance from the surface to the ambient is

$$R \equiv \frac{T_o - T_s}{Q/A} \quad (A3)$$

where  $T_s$  is defined in Figure 24B.

To transform (A2) into the form of (A3), the term

$$\frac{1}{A} \int_A h T_s dA$$

can be subtracted from and added to the second and third terms of (A2), respectively to yield:

$$Q/A = (T_o - T_s) h_{av} - \frac{1}{A} \int_A (T_c - T_s) h dA . \quad (A4)$$

Thus we now have:

$$R = \frac{1}{h_{av}} + \frac{1}{Q} \int_A \frac{h}{h_{av}} (T_c - T_s) dA . \quad (A5)$$

The second term on the right-hand side of (A5) is the constriction resistance:

$$R_c \equiv \frac{1}{Q} \int \frac{h}{h_{av}} (T_c - T_s) dA . \quad (A5.A)$$

This represents the difference in total resistance between the two cases pictured in Figure 25A.

Figure 25B illustrates the basic model for which Equation (5) was developed. At  $z = 0$ ,  $h$  is a function of radius, and the sides are insulated. Also,  $\frac{\partial T}{\partial z} = \text{constant}$  as  $z \rightarrow \infty$ .

The governing differential equation for the situation is

$$\nabla^2 T = 0 \quad (A6)$$

where  $\nabla^2$  is the Laplacian operator. For the given boundary conditions, the steady-state solution is

$$T_s = T_c - \frac{Q}{k\pi b^2} z + \sum_{n=1}^{\infty} C_n e^{-v_n z/b} J_0(v_n r/b) \quad (A7)$$

where  $v_n$  are the roots of

$$J_1(v_n) = 0 . \quad (A8)$$

Using relation (A8) and the approximation

$$\frac{[-k(\frac{\partial T}{\partial z})_{z=0}]_{\text{at } r}}{Q/A} \approx \frac{h(r)}{h_{av}} , \quad (A9)$$

Equation (A7) becomes

$$T_c - T_s = \frac{2Q}{\pi b k} \sum_{n=1}^{\infty} \frac{\int_0^1 \lambda J_0(v_n \lambda) f(\lambda) d\lambda}{v_n J_0^2(v_n)} J_0(v_n \lambda) \quad (A10)$$

where  $\lambda \equiv r/b$  and  $f(\lambda) \equiv h/h_{av}$ . Combining (A5.A) and (A10) will yield

$$R_c = 4 \frac{b}{k} \sum_{n=1}^{\infty} \frac{[\int_0^1 \lambda f(\lambda) J_0(v_n \lambda) d\lambda]^2}{v_n J_0^2(v_n)} \quad (A11)$$

Contact conductance for purely rough surfaces with Gaussian surface height distributions has been shown in Reference [2] to be

$$h_c = 1.45 \frac{k \tan \theta}{\sigma} \left( \frac{P_a}{H} \right)^{0.985} \quad (A12)$$

where the variables have been defined in the nomenclature. By combining (A11) and (A12), Equation (A5) becomes Equation 5:

$$R = 0.345 \frac{\sigma}{k \tan \theta} \left[ \int_0^1 \lambda \left( \frac{P}{H} \right)^{0.985} d\lambda \right]^{-1} + \frac{8b}{k} \sum_{n=1}^{\infty} \frac{[\int_0^1 \lambda (P/P_{av})^{0.985} J_0(v_n \lambda) d\lambda]^2}{v_n J_0^2(v_n)} \quad (5)$$

APPENDIX B  
COMPUTER PROGRAMS

List of Fortran Variables Used in Programs

<u>Notation of This Thesis</u>	<u>Fortran Symbol</u>
$a_H$	AH
$\overline{a}_H$	AHB
b	B
$\overline{F}$	PLOAD, FBAR
H	H
$J_0(x)$	BESEL(X)
k	AK
p, or P	PRES, PRSS, PREZ, HRTZP (Hertzian) PRESH (Due to Hertzian Y)
$\overline{p}$ , or $\overline{P}$	PBAR, PBAZ
Pl	PL
R	RES
$R_1$	RADI, RAD
$R_1, R_2$	R1, R2
r	R, RR, RHOM (radial position of dA)
$\overline{r}, d\overline{r}$	RB, DRB
$\overline{Y}(\overline{r})$	YB(I)
$\overline{Y}(0)$	YNB
$\lambda, d\lambda$	ALAM, DL
$v_n$ where $J_1(v_n) = 0$	ANU(J)

Notation of This Thesis

Fortran Symbol

$\rho$   $\bar{\rho}$

S

Tan $\theta$

TAN

Tan<sub>1</sub> $\theta$ , Tan<sub>2</sub> $\theta$

TAN1, TAN2

$\sigma$

SIGMA

$\sigma_1, \sigma_2$

SIGM1, SIGM2

PROGRAM TO DETERMINE DIMENSIONLESS PRESSURE  
DISTRIBUTIONS BETWEEN ROUGH AND WAVY SURFACES

INPUT DATA	LINE NO.
a. MAX = Number of radial increments	31
b. $P_l, \bar{F}$	33
c. YNB = first approximation for $\bar{Y}(0)$	38
OUTPUT DATA	
a. $P_l, \bar{F}$	41
b. Dimensionless Hertzian pressures	57
c. Dimensionless Hertzian radius	68
d. First approximation for $\bar{Y}(\bar{r})$	69
e. First approximation for $\bar{P}(\bar{r})$	78
f. Second approximation for $\bar{P}(\bar{r})$	96
g. If any values of $\bar{Y}(\bar{r})$ are negative, they are written here.	151
h. Final values, $\bar{P}(\bar{r})$	229
i. Final values, $\bar{Y}(\bar{r})$	230
j. $\bar{F}$ calculated from $\bar{P}(\bar{r})$	232
k. Dimensionless radial coordinates	235
l. $P_l, \bar{F}$	239



```

8010 CONTINUE
      READ(5,112) YNR
8000 CONTINUE
      WRITE(6,117)
      WRITE(6,118) PL,FBAR
      DO 75 I=1,MAX
75    PRSS(I)=0.0
      PLJAD=FBAR
      RMAX=MAX-1
      MAXM1=MAX-1
      AHR=1.333*((FBAR/PL)**.3333)
      AH=AHR
      AHSQ=AHB*AHB
      LL=(RMAX/4.0)+1.5
      DRB=(4.0*AHB)/RMAX
      DO 491 I=1,LL
491    RB=FLOAT(I-1)*DRB
      HRTZP(I)=.477*(FBAR/AHSQ)*SQRT(1.0-(RB*RB/AHSQ))
      CONTINUE
      WRITE(6,480)
      WRITE(6,103) (HRTZP(I),I=1,LL)
      DO 1 I=1,MAX
1    RB=FLOAT(I-1)*DRB
      IF(RB-AHB)4,4,5
4    YB(I)=0.0
      GO TO 1
5    SIDE=SQRT(RB*RB-AHSQ)
      Y3(I)=.5*(RB*RB-2.0*AHSQ*(1.0-.318*((2.0-((RB/AH)**2.0))*ATAN(AH/
1SIDE)+((RB*RB)/(AHSQ))-1.0)**0.5)))
      CONTINUE
      WRITE(6,105)
      WRITE(6,102) AHR
      WRITE(6,103) (YB(I),I=1,MAX)
      DO 200 I=1,MAX
200    PRES(I)=0.5*(1.0-ERF(YB(I)/(1.414)))
      PSTEST=.001*PRES(1)
PRES0037
PRES0038
PRES0039
PRES0040
PRES0041
PRES0042
PRES0043
PRES0044
PRES0045
PRES0046
PRES0047
PRES0048
PRES0049
PRES0050
PRES0051
PRES0052
PRES0053
PRES0054
PRES0055
PRES0056
PRES0057
PRES0058
PRES0059
PRES0060
PRES0061
PRES0062
PRES0063
PRES0064
PRES0065
PRES0066
PRES0067
PRES0068
PRES0069
PRES0070
PRES0071
PRES0072

```



```

200 IF(PRESH(I).LT.PTEST) GO TO 1984
    CONTINUE
1984 MAX=I
    MAXM1=MAX-1
    WRITE(6,1011)
    WRITE(6,103) (PRESH(I),I=1,MAX)
    TEST1=.01*PRESH(1)
    AEAR=0.0
    DO 486 I=1,MAX
        R8=FLOAT(I-1)*DRR
        AEAR=AEAR+PRESH(I)*R8*DRR
        FLOAD=2.0*PI*AEAR
        GO TO 195
1898 CONTINUE
    G=G+1.0
    IF(G.EQ.1.0) GO TO 8001
    GO TO 8003
8001 CONTINUE
    DO 8002 I=1,MAX
        PBAR(I)=(HRTZP(I)+PBAR(I))/2.0
        PR1(I)=PBAR(I)
8002 CONTINUE
    WRITE(6,4756)
    WRITE(6,103) (PBAR(I),I=1,MAX)
8003 CONTINUE
    DO 8004 I=1,MAX
        PBAR(I)=(PR1(I)+PBAR(I))/2.0
        PR1(I)=PBAR(I)
8004 CONTINUE
    TEST1=.01*PBAR(1)
    COUNT=COUNT+1.0
    IF(COUNT-15.0)1972,1972,1979
1972 CONTINUE
    DO 85 I=1,MAX
        PRSS(I)=PBAR(I)
85 TEST=0.1*PBAR(1)

```

```

PRES0073
PRES0074
PRES0075
PRES0076
PRES0077
PRES0078
PRES0079
PRES0080
PRES0081
PRES0082
PRES0083
PRES0084
PRES0085
PRES0086
PRES0087
PRES0088
PRES0089
PRES0090
PRES0091
PRES0092
PRES0093
PRES0094
PRES0095
PRES0096
PRES0097
PRES0098
PRES0099
PRES0100
PRES0101
PRES0102
PRES0103
PRES0104
PRES0105
PRES0106
PRES0107
PRES0108

```

```

N=MAX
AREA=C.0
DO 25 I=2,N
RB=FLOAT(I-1)*DRB
SUM=0.0
ADD=2.0*SQRTP(PI)*DRB*PBAR(I)
DO 26 K=1,N
RHOM=FLOAT(K-1)*DRB
SUM1=(2.0*RHOM*DRB*PBAR(K))/(RHOM*RHOM+RB*RB)**.5
EP=2.0*RB*RHOM/(RB*RB+RHOM*RHOM)
IF(EP-1.0)600,601,601
S3=0.0
DO 300 J=1,5
THETA=FLOAT(J-1)*PI/90.0+PI/180.0
S=SQRTP(1.0-EP*COS(THETA))
S3=S3+(PI/90.0)/S
CONTINUE
S4=0.0
DO 301 M=2,18
THETA=FLOAT(M-1)*PI/18.0+PI/36.0
S=SQRTP(1.0-EP*COS(THETA))
S4=S4+(PI/18.0)/S
CONTINUE
S1=S3+S4
GO TO 602
S1=(2.0*.5)*ALOG(8.0*RB/DRB)
SUM=SUM+(SUM1*S1)
CONTINUE
W(I)=(SUM+ADD)/PL
W(1)=W(2)+(DRB*DRB)/2.0
AEAP=0.0
DO 50 I=1,MAX
RB=FLOAT(I-1)*DRB
RTER(I)=RB*RB/2.0
YB(I)=RTER(I)-W(1)+W(I)+YNB
PBAR(I)=0.5*(1.0-ERF(YB(I)/(2.0**.5)))

```

600

300

301

601

602

26

25

PRES0109

PRES0110

PRES0111

PRES0112

PRES0113

PRES0114

PRES0115

PRES0116

PRES0117

PRES0118

PRES0119

PRES0120

PRES0121

PRES0122

PRES0123

PRES0124

PRES0125

PRES0126

PRES0127

PRES0128

PRES0129

PRES0130

PRES0131

PRES0132

PRES0133

PRES0134

PRES0135

PRES0136

PRES0137

PRES0138

PRES0139

PRES0140

PRES0141

PRES0142

PRES0143

PRES0144

```

50      CONTINUE
      DO 950 I=1, MAX
      IF(YB(I).LT.0.0) GO TO 8880
950     CONTINUE
      GO TO 1099
8880     CONTINUE
      WRITE(6,103) (YB(I),I=1,MAX)
482     CONTINUE
483     CONTINUE
      DO 484 I=1, MAX
      P3AR(I)=0.5*(1.0-ERF(YB(I)/(2.0**.5)))
484     CONTINUE
      GO TO 1099
195     CONTINUE
495     CONTINUE
      DO 295 I=1, MAX
      AEAP=0.0
      Y3(I)=YB(I)+YNB
      DO 99 I=1, MAX
      PBAR(I)=0.5*(1.0-ERF(YB(I)/(2.0**.5)))
99      CONTINUE
1099     CONTINUE
      DO 97 I=1, MAX
      IF(A3S(PRSS(I)-PBAR(I)).GT.TEST1) GO TO 75
97      CONTINUE
      AF=(FLOAD-PLoad)/PLoad
      IF(ABS(AF).GT.0.1) GO TO 76
      GO TO 16
76      CONTINUE
      DO 44 I=1, MAXM1
      RB=FLOAT(I-1)*DRB
      AEAP=AEAP+PRAR(I)*R3*DRB
44      FLOAD=2.0*PI*AEAP+(PBAR(1)*PI*DRB*DRB)/4.0
      AF=(FLOAD-PLoad)/PLoad
      AEAZ=0.0
      DO 196 I=1, MAX

```

```

PRES0145
PRES0146
PRES0147
PRES0148
PRES0149
PRES0150
PRES0151
PRES0152
PRES0153
PRES0154
PRES0155
PRES0156
PRES0157
PRES0158
PRES0159
PRES0160
PRES0161
PRES0162
PRES0163
PRES0164
PRES0165
PRES0166
PRES0167
PRES0168
PRES0169
PRES0170
PRES0171
PRES0172
PRES0173
PRES0174
PRES0175
PRES0176
PRES0177
PRES0178
PRES0179
PRES0180

```

```

196      Z(I)=YB(I)-YB(1)
      PBAZ(I)=0.5*(1.0-ERF(Z(I)/(2.0**.5)))
      CONTINUE
      DO 190 I=1,MAXM1
      RB=FLOAT(I-1)*DRB
      AEAZ=AEAZ+PBAZ(I)*RB*DRB
190      FLJAZ=2.0*PI*AEAZ+(PBAZ(I)*PI*DRB*DRB)/4.0
      CHECK=FLJAZ-PLJAD
      DO 5000 I=1,MAX
5000      YB(I)=Z(I)
      IF(CHECK)GO11,9011,192
9011      CONTINUE
      DO 9012 I=1,MAX
      PRAR(I)=PBAZ(I)
9012      CONTINUE
9013      CONTINUE
      GO TO 11
192      IF(PLJAD.GT.FLJAD) GO TO 193
      GO TO 191
193      AF=(FLOAD-PLJAD)/PLOAD
      IF(ABS(AF).LT.0.1) GO TO 1898
      IF(ABS(AF).LT.0.4) GO TO 476
      IF(ABS(AF).LT.0.6) GO TO 470
      IF(ABS(AF).LT.1.0) GO TO 477
      YNR=YNB*0.8
      GO TO 471
476      YNR=YNB*0.99
      GO TO 471
470      YNB=YNB*0.96
      GO TO 471
477      YNR=YNB*0.90
471      CONTINUE
      GO TO 195
191      AF=(FLOAD-PLJAD)/PLOAD
      IF(ABS(AF).LT.0.1) GO TO 1898
      IF(ABS(AF).LT.0.4) GO TO 478

```

PRES0181  
 PRES0182  
 PRES0183  
 PRES0184  
 PRES0185  
 PRES0186  
 PRES0187  
 PRES0188  
 PRES0189  
 PRES0190  
 PRES0191  
 PRES0192  
 PRES0193  
 PRES0194  
 PRES0195  
 PRES0196  
 PRES0197  
 PRES0198  
 PRES0199  
 PRES0200  
 PRES0201  
 PRES0202  
 PRES0203  
 PRES0204  
 PRES0205  
 PRES0206  
 PRES0207  
 PRES0208  
 PRES0209  
 PRES0210  
 PRES0211  
 PRES0212  
 PRES0213  
 PRES0214  
 PRES0215  
 PRES0216

```
IF (ABS(AF).LT.0.6) GO TO 473
IF (ABS(AF).LT.1.0) GO TO 479
YNB=YNB*1.2
GO TO 474
478 YNB=YNB*1.01
GO TO 474
473 YNB=YNB*1.04
GO TO 474
479 YNB=YNB*1.1
474 CONTINUE
GO TO 195
16 WRITE(6,109)
WRITE(6,103) (PBAR(I),I=1,MAX)
WRITE(6,103) (YB(I),I=1,MAX)
WRITE(6,107)
WRITE(6,108) FLOAD
DO 1970 I=1,MAX
RADIM=FLOAD*(I-1)*DRB
WRITE(6,103) RADIM
1970 CONTINUE
1979 CONTINUE
WRITE(6,117)
WRITE(6,118) PL,PBAR
1973 CONTINUE
1978 CONTINUE
4901 CONTINUE
1971 CALL EXIT
END
PRES0217
PRES0218
PRES0219
PRES0220
PRES0221
PRES0222
PRES0223
PRES0224
PRES0225
PRES0226
PRES0227
PRES0228
PRES0229
PRES0230
PRES0231
PRES0232
PRES0233
PRES0234
PRES0235
PRES0236
PRES0237
PRES0238
PRES0239
PRES0240
PRES0241
PRES0242
PRES0243
PRES0244
```

PROGRAM TO DETERMINE CONTACT RESISTANCE  
USING EQUATION (5)

INPUT DATA	LINE NO.
a. $H, \sigma_1, \sigma_2, \tan_1 \theta, \tan_2 \theta$	34
b. $k$ (thermal conductivity)	35
c. $R_1, R_2, \text{MAX} = \text{Number of pressures to be read}$ in, $N = \text{number of roots of } J_1(v_n) = 0 \text{ to be read in}$	36
d. Dimensionless pressures	37
e. Roots of $J_1(v_n) = 0$	38
f. Dimensionless radial increment	39
g. Average pressure $\equiv F/A_{\text{app}}$	40
OUTPUT DATA	
a. INPUT DATA	93-100
b. Microscopic resistance term	102
c. Macroscopic resistance term	104
d. Total contact resistance	106

NOTE: The number appearing in the inequality in card 107 should be one less than the number of sets of input data.

```

C      FUNCTION RESEL(X)
C      *****
C      BESSEL FUNCTION SUB-ROUTINE USED IN THE PROGRAM FOR CONTACT RESIS-
C      TANCE USING EQUATION (5)
C      *****
C      IF(X-3.0)10,10,11
C      RESEL=1.0-2.24999*((X/3.0)**2.0)+1.26562*((X/3.0)**4.0)-.31638*((X
10    1/3.0)**6.0)+.04444*((X/3.0)**8.0)-.00394*((X/3.0)**10.0)+.00021*((
    1X/3.0)**12.0)
C      RETURN
C      FZ=.79788-.00552*((3.0/X)**2.0)-.00009*((3.0/X)**3.0)+.00137*((3.0
11    1/X)**4.0)-.00072*((3.0/X)**5.0)+.00014*((3.0/X)**5.0)
    THETA=X-.78539-.04166*(3.0/X)-.00004*((3.0/X)**2.0)+.00263*((3.0/X
    1)**3.0)-.00054*((3.0/X)**4.0)-.00029*((3.0/X)**5.0)+.00014*((3.0/X
    1)**6.0)
    BESEL=(FZ*COS(THETA))/(X**0.5)
    RETURN
END

```

```

RESI00001
RESI00002
RESI00003
RESI00004
RESI00005
RESI00006
RESI00007
RESI00008
RESI00009
RESI00010
RESI00011
RESI00012
RESI00013
RESI00014
RESI00015
RESI00016
RESI00017
RESI00018
RESI00019
RESI00020
RESI00021
RESI00022
RESI00023
RESI00024
RESI00025
RESI00026
RESI00027
RESI00028
RESI00029
RESI00030
RESI00031
RESI00032
RESI00033
RESI00034
RESI00035
RESI00036

DIMENSION PRAR(200),PRES(200),ANU(200)
*****
PROGRAM TO DETERMINE THERMAL CONTACT RESISTANCE USING EQUATION (5)
*****
      FFORMAT(5E15.4)
      FFORMAT(2E15.4,2I10)
      FFORMAT(6F10.4)
      FFORMAT(1H,6X,1HH,8X,5HSIGM1,10X,5HSIGM2/)
      FFORMAT(3F15.4)
      FFORMAT(1H,4HTAN1,10X,4HTAN2,11X,1HK/)
      FFORMAT(5X,3HMAX,5X,1HN,5X,2HR1,13X,2HR2/)
      FFORMAT(1H,17,I6,2E15.4)
      FFORMAT(1H,23HDIMENSIONLESS PRESSURES/)
      FFORMAT(1H,18HCONTACT RESISTANCE/)
      FFORMAT(1H,E15.4,1X,16H(HR-F-FT-FT)/8TU/)
      FFORMAT(E15.4)
      FFORMAT(1H,4HDRB=,E15.4)
      FFORMAT(1H,E15.4)
      FFORMAT(23HMAXP IS GREATER THAN LB/)
      FFORMAT(1X,10HSIGMA TERM/)
      FFORMAT(1X,6HB TERM/)
      FFORMAT(1X,17HAVERAGE PRESSURE=,E15.4/)
      FFORMAT(E15.4)
      FFORMAT(1X,6HP/PAV=)
      FFORMAT(1H,5X,2HY=,9X,10HJ-ZERO(Y)=)
      FFORMAT(2E15.4)
      FFORMAT(F15.2)
      B=0.5
      BNUM=0.0
      CONTINUE
      BNUM=BNUM+1.0
      READ(5,100) H,SIGM1,SIGM2,TAN1,TAN2
      READ(5,117) AK
      READ(5,101) R1,R2,MAX,N

```



```

READ(5,100) (PBAR(I),I=1,MAX)
READ(5,103) (ANU(J),J=1,N)
READ(5,115) DR
READ(5,135) PAV
PTOT=0.0
TAN=(TAN1*TAN1+TAN2*TAN2)**0.5
SIGMA=(SIGM1*SIGM1+SIGM2*SIGM2)**0.5
RADI=(R1*R2)/(R1+R2)
DR=DR8*((RADI*SIGMA)**0.5)
MAXP=MAX+1
LB=B/DR
IF(LB-MAXP)51,51,49
CONTINUE
DO 50 I=MAXP,LB
PBAR(I)=0.0
CONTINUE
GO TO 52
51 CONTINUE
WRITE(6,118)
52 CONTINUE
MAX=LB
PAVI=0.0
DO 2 K=1,MAX
RR=FLOAT(K-1)*DR
PRES(K)=H*PBAR(K)
PAVI=PAVI+PRES(K)*RR*DR
CONTINUE
WRITE(6,130) PAV
CK2=(0.345*SIGMA)/(AK*TAN)
CK3=(8.0*R)/AK
SUM=0.0
DO 3 I=1,MAX
R=FLOAT(I-1)*DR
ALAM=R/R
DL=DR/R
SUM=SUM+ALAM*(PBAR(I)**0.985)*DL
2
3

```

RES10037  
RFS10038  
RES10039  
RES10040  
RES10041  
RES10042  
RES10043  
RES10044  
RES10045  
RES10046  
RES10047  
RFS10048  
RES10049  
RES10050  
RES10051  
RES10052  
RES10053  
RES10054  
RES10055  
RES10056  
RES10057  
RES10058  
RES10059  
RFS10060  
RES10061  
RES10062  
RFS10063  
RES10064  
RES10065  
RES10066  
RFS10067  
RFS10068  
RES10069  
RES10070  
RES10071  
RFS10072

```

3  CONTINUE
   TERM1=CK2/SUM
   SUMMA=0.0
   DO 5 J=1,N
     X=ANU(J)
     SUM1=0.0
     DO 4 I=1,MAX
       R=FLJAT(I-1)*DR
       ALAM=R/B
       Y=ANJ(J)*ALAM
       SUM1=SUM1+ALAM*((PRES(I)/PAV)**0.985)*(BESEL(Y))*DL
4    CONTINUE
     SUMMA=SUMMA+(SUM1*SUM1)/(ANU(J)*(ABS(BESEL(X))*2.0))
     WRITE(6,131) SUM1
5    CONTINUE
     TERM2=CK3*SUMMA
     RES=(TERM1+TERM2)/12.0
     ANS1=TERM1/12.0
     ANS2=TERM2/12.0
     WRITE(6,104)
     WRITE(6,106) H,SIGM1,SIGM2
     WRITE(6,116) DRB
     WRITE(6,107)
     WRITE(6,106) TAN1,TAN2,AK
     WRITE(6,108)
     WRITE(6,109) MAX,V,R1,R2
     WRITE(6,110)
     WRITE(6,100) (PRAR(I),I=1,MAX)
     WRITE(6,119)
     WRITE(6,112) ANS1
     WRITE(6,120)
     WRITE(6,112) ANS2
     WRITE(6,111)
     WRITE(6,112) RES
     IF(RVUM.GT.6.0) GO TO 3334
     GO TO 3333
RESI0073
RESI0074
RESI0075
RESI0076
RESI0077
RESI0078
RESI0079
RESI0080
RESI0081
RESI0082
RESI0083
RESI0084
RESI0085
RESI0086
RESI0087
RESI0088
RESI0089
RESI0090
RESI0091
RESI0092
RESI0093
RESI0094
RESI0095
RESI0096
RESI0097
RESI0098
RESI0099
RESI0100
RESI0101
RESI0102
RESI0103
RESI0104
RESI0105
RESI0106
RESI0107
RESI0108

```

```

3334 CONTINUE
C K IS IN (RTU/HR-F-FT)
C SIGMA AND R ARE IN INCHES
C RESISTANCE IS IN (HR-F-FT-FT)/RTU
CALL EXIT
END

```

```

RESI0109
RESI0110
RESI0111
RESI0112
RESI0113
RESI0114

```

APPENDIX C

TABLES OF COORDINATES FOR PRESSURE DISTRIBUTIONS

$P_1 = .002$

$\overline{F} = .005$

$\overline{r}$	$\overline{F}$
0.000	.00066
0.302	.00066
0.603	.00061
0.905	.00054
1.206	.00046
1.508	.00034
1.809	.00019
2.111	.00007
2.412	.00000

P1 = .004

$\bar{F} = .005$

$\bar{F} = .010$

$\bar{r}$	$\bar{P}$	$\bar{r}$	$\bar{P}$
0.000	.00097	0.000	.00132
0.239	.00097	0.302	.00132
0.478	.00089	0.603	.00121
0.718	.00081	0.905	.00109
0.957	.00068	1.206	.00092
1.197	.00052	1.508	.00069
1.436	.00034	1.809	.00040
1.675	.00016	2.111	.00014
1.915	.00005	2.412	.00002
2.154	.00001	2.714	.00000
2.393	.00000		

P1 = .006

$\bar{F} = .010$

$\bar{F} = .015$

$\bar{r}$	$\bar{P}$	$\bar{r}$	$\bar{P}$
0.000	.00164	0.000	.00199
0.263	.00164	0.302	.00199
0.527	.00152	0.603	.00183
0.790	.00136	0.905	.00165
1.054	.00115	1.206	.00139
1.317	.00087	1.508	.00103
1.580	.00054	1.809	.00062
1.844	.00024	2.111	.00023
2.107	.00006	2.412	.00004
2.371	.00000	2.714	.00000

$$P1 = .01$$

$$\overline{F} = .02$$

$\overline{r}$	$\overline{P}$
0.000	.00293
0.279	.00293
0.559	.00270
0.839	.00243
1.120	.00204
1.400	.00153
1.679	.00093
1.959	.00039
2.239	.00009
2.519	.00000

P1 = .02

$\bar{F} = .040$

$\bar{F} = .060$

$\bar{r}$	$\bar{P}$	$\bar{r}$	$\bar{P}$
0.000	.00590	0.000	.00685
0.279	.00590	0.320	.00685
0.559	.00545	0.641	.00631
0.839	.00492	0.961	.00568
1.120	.00416	1.282	.00476
1.400	.00316	1.602	.00350
1.679	.00199	1.922	.00198
1.959	.00089	2.243	.00068
2.239	.00023	2.563	.00010
2.519	.00003	2.884	.00000
2.799	.00000		

$\bar{F} = .080$

$\bar{r}$	$\bar{P}$
0.000	.00765
0.353	.00765
0.705	.00701
1.058	.00629
1.411	.00528
1.763	.00384
2.116	.00203
2.469	.00054
2.821	.00005



P1 = .04

$\bar{F} = .13$		$\bar{F} = .16$	
$\bar{r}$	$\bar{P}$	$\bar{r}$	$\bar{P}$
0.000	.01412	0.000	.01556
0.320	.01412	0.353	.01556
0.641	.01305	0.705	.01433
0.961	.01182	1.058	.01294
1.282	.01004	1.411	.01090
1.602	.00763	1.763	.00807
1.922	.00469	2.116	.00458
2.243	.00189	2.469	.00145
2.563	.00036	2.821	.00016
2.884	.00002	3.174	.00000
3.204	.00000		

P1 = .05

$\bar{F}$  = .2

$\bar{r}$	$\bar{p}$
0.000	.01861
0.353	.01861
0.705	.01708
1.058	.01530
1.411	.01273
1.763	.00916
2.116	.00487
2.469	.00140
2.821	.00014
3.174	.00000
3.527	.00000

P1 = .1

$\bar{F} = .25$

$\bar{r}$	$\bar{p}$
0.000	.03056
0.302	.03056
0.603	.02825
0.905	.02540
1.206	.02138
1.508	.01609
1.809	.00992
2.111	.00429
2.412	.00104
2.714	.00011
3.015	.00000

$\bar{F} = .5$

$\bar{r}$	$\bar{p}$
0.000	.04072
0.367	.04072
0.734	.03758
1.100	.03397
1.467	.02878
1.834	.02169
2.201	.01282
2.567	.00439
2.934	.00053
3.301	.00002
3.668	.00000

$\bar{F} = .6$

$\bar{r}$	$\bar{p}$
0.000	.04503
0.415	.04503
0.829	.04122
1.244	.03693
1.658	.03079
2.073	.02210
2.488	.01103
2.902	.00232
3.317	.00009
3.731	.00000

P1 = .20

$\bar{F} = .2$

$\bar{r}$	$\bar{P}$
0.000	.03741
0.222	.03741
0.444	.03543
0.667	.03010
0.889	.02685
1.111	.02071
1.333	.01446
1.555	.00859
1.777	.00409
1.999	.00145
2.222	.00036
2.444	.00006
2.666	.00000

$\bar{F} = .4$

$\bar{r}$	$\bar{P}$
0.000	.05564
0.280	.05564
0.560	.05174
0.840	.04685
1.120	.04008
1.400	.03131
1.679	.02105
1.959	.01096
2.239	.00378
2.519	.00073
2.799	.00007
3.079	.00000

$\bar{F} = .6$

$\bar{r}$	$\bar{P}$
0.000	.06558
0.320	.06558
0.641	.06071
0.961	.05472
1.282	.04625
1.602	.03506
1.922	.02189
2.243	.00954
2.563	.00223
2.884	.00021
3.204	.00000

$\bar{F} = .8$

$\bar{r}$	$\bar{P}$
0.000	.07312
0.353	.07312
0.705	.06748
1.058	.06068
1.411	.05091
1.763	.03767
2.116	.02191
2.469	.00788
2.821	.00119
3.174	.00005
3.527	.00000

P1 = .20

$\bar{F} = 1$

$\bar{r}$	$\bar{P}$
0.000	.08200
0.379	.08200
0.759	.07567
1.114	.06825
1.520	.05759
1.899	.04296
2.279	.02486
2.659	.00818
3.039	.00090
3.419	.00002
3.799	.00000

$\bar{F} = 1.3$

$\bar{r}$	$\bar{P}$
0.000	.09035
0.404	.09035
0.807	.08344
1.211	.07551
1.615	.06403
2.018	.04827
2.422	.02826
2.826	.00897
3.229	.00079
3.633	.00001
4.037	.00000

$\bar{F} = 1.4$

$\bar{r}$	$\bar{P}$
0.000	.09551
0.425	.09551
0.850	.08810
1.275	.08002
1.700	.06825
2.125	.05113
2.550	.02863
2.975	.00791
3.400	.00049
3.825	.00000

$\bar{F} = 1.6$

$\bar{r}$	$\bar{P}$
0.000	.09919
0.444	.09919
0.889	.09136
1.333	.08232
1.777	.06892
2.222	.05033
2.666	.02679
3.110	.00611
3.554	.00023
3.999	.00000

$$P1 = .20$$

$$\overline{F} = 1.7$$

$\overline{r}$	$\overline{P}$
0.000	.10280
0.462	.10280
0.924	.09467
1.386	.08538
1.848	.07131
2.310	.05126
2.773	.02578
3.235	.00489
3.697	.00011
4.159	.00000

P1 = .30

$\bar{F} = .2$

$\bar{F} = .4$

$\bar{r}$	$\bar{p}$	$\bar{r}$	$\bar{p}$
0.000	.04341	0.000	.06279
0.194	.04341	0.245	.06279
0.388	.04109	0.489	.05844
0.582	.03840	0.734	.05259
0.776	.03203	0.978	.04461
0.970	.02575	1.223	.03477
1.164	.01922	1.467	.02403
1.359	.01283	1.712	.01364
1.553	.00742	1.956	.00588
1.747	.00357	2.201	.00174
1.941	.00137	2.445	.00032
		2.690	.00003
		2.934	.00000

$\bar{F} = .6$

$\bar{F} = .8$

$\bar{r}$	$\bar{p}$	$\bar{r}$	$\bar{p}$
0.000	.07933	0.000	.10440
0.280	.07933	0.308	.10440
0.559	.07374	0.616	.10020
0.837	.06653	0.924	.08434
1.120	.05658	1.232	.06819
1.400	.04384	1.540	.05281
1.679	.02921	1.848	.03449
1.959	.01511	2.157	.01671
2.239	.00525	2.465	.00484
2.519	.00103	2.773	.00066
2.799	.00099	3.081	.00003
3.079	.00000	3.389	.00000

P1 = .30

$\bar{F} = 1.2$

$\bar{F} = 1.5$

$\bar{r}$	$\bar{P}$	$\bar{r}$	$\bar{P}$
0.000	.11040	0.000	.11940
0.353	.11040	0.379	.11940
0.705	.10230	0.759	.11030
1.058	.09235	1.140	.09936
1.411	.07819	1.520	.08357
1.763	.05913	1.899	.06189
2.116	.03619	2.279	.03556
2.469	.01456	2.659	.01198
2.821	.00268	3.039	.00144
3.174	.00015	3.419	.00004
3.527	.00000	3.799	.00000

$\bar{F} = 2$

$\bar{F} = 2.6$

$\bar{r}$	$\bar{P}$	$\bar{r}$	$\bar{P}$
0.000	.13300	0.000	.15240
0.418	.13300	0.450	.15240
0.836	.12230	0.901	.14070
1.254	.11000	1.351	.12800
1.672	.09227	1.802	.10950
2.091	.06731	2.252	.08245
2.509	.03580	2.702	.04636
2.927	.00912	3.153	.01238
3.345	.00054	3.603	.00060
3.736	.00000	4.054	.00000



P1 = .30

$\bar{F} = 3.1$

$\bar{F} = 3.4$

$\bar{r}$	$\bar{p}$	$\bar{r}$	$\bar{p}$
0.000	.19610	0.000	.16930
0.479	.19610	0.499	.16930
0.957	.18000	0.998	.15550
1.436	.15500	1.497	.14050
1.914	.12160	1.996	.11900
2.393	.08924	2.495	.08791
2.872	.04903	2.994	.04557
3.350	.01158	3.493	.00824
3.829	.00035	3.992	.00012
4.307	.00000	4.491	.00000

P1 = .40

$\bar{F} = .1$		$\bar{F} = .2$	
$\bar{r}$	$\bar{P}$	$\bar{r}$	$\bar{P}$
0.000	.02907	0.000	.04654
0.140	.02907	0.176	.04654
0.279	.02770	0.353	.04411
0.419	.02567	0.529	.04010
0.559	.02301	0.705	.03503
0.699	.01985	0.882	.02884
0.839	.01638	1.058	.02233
0.979	.01281	1.234	.01584
1.120	.00941	1.411	.01008
1.260	.00644	1.587	.00561
1.400	.00405	1.763	.00265
1.540	.00231	1.940	.00103
1.680	.00118	2.116	.00032
1.820	.00054	2.292	.00008
1.959	.00021	2.469	.00001
2.099	.00007	2.645	.00000
2.239	.00002		
2.379	.00000		

P1 = .40

$\bar{F} = .3$		$\bar{F} = .4$	
$\bar{r}$	$\bar{p}$	$\bar{r}$	$\bar{p}$
0.000	.05887	0.000	.07284
0.202	.05887	0.222	.07284
0.404	.05519	0.444	.06905
0.606	.05004	0.667	.04606
0.807	.04320	0.889	.05324
1.009	.03497	1.111	.04192
1.211	.02603	1.333	.03019
1.413	.01720	1.555	.01883
1.615	.00972	1.777	.00963
1.817	.00450	1.999	.00378
2.019	.00162	2.222	.00106
2.220	.00044	2.444	.00020
2.422	.00008	2.666	.00002
2.624	.00001	2.888	.00000
2.826	.00000		

P1 = .40

$\bar{F} = .5$

$\bar{F} = 1.0$

$\bar{r}$	$\bar{P}$	$\bar{r}$	$\bar{P}$
0.000	.07819	0.000	.14330
0.239	.07819	0.302	.14330
0.479	.07288	0.603	.13600
0.718	.06563	0.905	.12600
0.957	.05584	1.206	.09847
1.197	.04382	1.508	.07404
1.436	.03064	1.809	.04977
1.675	.01795	2.111	.02613
1.915	.00819	2.412	.00886
2.154	.00267	2.714	.00154
2.393	.00057	3.015	.00011
2.633	.00007	3.317	.00000
2.872	.00000		

$\bar{F} = 1.6$

$\bar{F} = 2.0$

$\bar{r}$	$\bar{P}$	$\bar{r}$	$\bar{P}$
0.000	.16620	0.000	.16250
0.345	.16620	0.380	.16250
0.690	.15000	0.760	.15070
1.035	.13430	1.140	.13660
1.381	.10980	1.520	.11630
1.726	.08462	1.899	.08867
2.071	.05520	2.279	.05445
2.416	.02549	2.659	.02113
2.761	.00606	3.039	.00327
3.106	.00051	3.419	.00012
3.451	.00001	3.799	.00000
3.797	.00000		

P1 = .40

$\bar{F} = 2.3$

$\bar{F} = 3$

$\bar{r}$	$\bar{P}$	$\bar{r}$	$\bar{P}$
0.000	.16910	0.000	.18660
0.409	.16910	0.434	.18660
0.818	.15580	0.869	.17200
1.228	.13980	1.305	.15490
1.637	.11670	1.739	.13030
2.046	.08486	2.174	.09618
2.455	.04595	2.609	.05282
2.864	.01283	3.044	.01389
3.274	.00097	3.479	.00077
3.683	.00001	3.914	.00000
4.092	.00000		

$\bar{F} = 3.5$

$\bar{F} = 4.0$

$\bar{r}$	$\bar{P}$	$\bar{r}$	$\bar{P}$
0.000	.20270	0.000	.21280
0.462	.20270	0.487	.21280
0.924	.18720	0.973	.19570
1.386	.16970	1.459	.17680
1.848	.14390	1.946	.14950
2.310	.10610	2.432	.10930
2.773	.05679	2.919	.05533
3.235	.01355	3.405	.01040
3.697	.00051	3.892	.00020
4.159	.00000	4.378	.00000

P1 = .50

$\bar{F} = 0.1$		$\bar{F} = 0.2$	
$\bar{r}$	$\bar{P}$	$\bar{r}$	$\bar{P}$
0.000	.03035	0.000	.04989
0.130	.03035	0.164	.04989
0.260	.02906	0.327	.04730
0.390	.02716	0.491	.04357
0.520	.02259	0.654	.03869
0.650	.02155	0.819	.02909
0.780	.01712	0.982	.02375
0.910	.01395	1.146	.01934
1.039	.01119	1.310	.01312
1.169	.00808	1.473	.00802
1.299	.00546	1.637	.00432
1.429	.00342	1.801	.00201
1.559	.00197	1.964	.00079
1.689	.00103	2.128	.00025
1.819	.00049	2.292	.00007
1.949	.00020	2.455	.00001
2.079	.00008	2.619	.00000
2.209	.00002		
2.339	.00000		

P1 = .50

$\bar{F} = 0.3$		$\bar{F} = 0.4$	
$\bar{r}$	$\bar{P}$	$\bar{r}$	$\bar{P}$
0.000	.06450	0.000	.07678
0.187	.06450	0.206	.07678
0.375	.06118	0.413	.07269
0.562	.05880	0.619	.06960
0.750	.04869	0.825	.05661
0.937	.03417	1.031	.04537
1.124	.03037	1.237	.03365
1.312	.02100	1.444	.02217
1.499	.01288	1.650	.01248
1.686	.00677	1.856	.00572
1.874	.00294	2.062	.00203
2.061	.00102	2.269	.00053
2.249	.00027	2.475	.00009
2.436	.00005	2.681	.00001
2.623	.00000	2.887	.00000

P1 = .50

$\bar{F} = 0.5$		$\bar{F} = 1$	
$\bar{r}$	$\bar{p}$	$\bar{r}$	$\bar{p}$
0.000	.08860	0.000	.12320
0.222	.08860	0.279	.12320
0.444	.08396	0.559	.11450
0.666	.07700	0.839	.10280
0.889	.06489	1.112	.08680
1.111	.05131	1.400	.06657
1.333	.03720	1.679	.04418
1.555	.02347	1.959	.02282
1.777	.01222	2.239	.00806
1.999	.00492	2.519	.00165
2.222	.00143	2.799	.00017
2.444	.00028	3.079	.00000
2.666	.00003		
2.888	.00000		



P1 = .50

$\bar{F} = 1.6$

$\bar{F} = 2$

$\bar{r}$	$\bar{P}$	$\bar{r}$	$\bar{P}$
0.000	.16010	0.000	.18160
0.320	.16010	0.353	.18160
0.641	.14910	0.705	.16870
0.961	.13520	1.058	.15280
1.282	.11580	1.411	.13030
1.602	.09038	1.763	.10030
1.922	.05998	2.116	.06408
2.243	.02954	2.469	.02833
2.563	.00861	2.821	.00624
2.884	.00112	3.174	.00045
3.204	.00005	3.527	.00000
3.524	.00000		

$\bar{F} = 3$

$\bar{F} = 4$

$\bar{r}$	$\bar{P}$	$\bar{r}$	$\bar{P}$
0.000	.21710	0.000	.23810
0.404	.21710	0.443	.23810
0.807	.20130	0.889	.21990
0.211	.18240	1.333	.19850
1.615	.15520	1.777	.16740
2.018	.11810	2.222	.12400
2.422	.07195	2.666	.06894
2.826	.02652	3.110	.01859
3.229	.00334	3.554	.00101
3.633	.00007	3.999	.00000
4.037	.00000		

P1 = .50

$\bar{F} = 5.3$

$\bar{F} = 5.5$

$\bar{r}$	$\bar{p}$	$\bar{r}$	$\bar{p}$
0.000	.26970	0.000	.27400
0.497	.26970	0.485	.27400
0.994	.24820	0.969	.25380
1.491	.22350	1.455	.23050
1.988	.18800	1.940	.19600
2.485	.13720	2.425	.14760
2.982	.06998	2.909	.08466
3.479	.01309	3.394	.02249
3.976	.00023	3.879	.00083
4.473	.00000	4.364	.00000

P1 = .60

$\bar{F} = .5$

$\bar{F} = .9$

$\bar{r}$	$\bar{p}$	$\bar{r}$	$\bar{p}$
0.000	.09278	0.000	.13250
0.209	.09278	0.263	.13250
0.418	.08787	0.526	.12340
0.627	.08000	0.790	.11120
0.836	.06858	1.054	.09446
1.045	.05507	1.317	.07363
1.254	.04093	1.580	.05048
1.463	.02701	1.844	.02816
1.673	.01521	2.107	.01155
1.882	.00694	2.371	.00307
2.091	.00244	2.634	.00047
2.300	.00062	2.897	.00004
2.509	.00011	3.161	.00000
2.718	.00001		
2.927	.00000		

$\bar{F} = 1.4$

$\bar{F} = 2.2$

$\bar{r}$	$\bar{p}$	$\bar{r}$	$\bar{p}$
0.000	.16470	0.000	.24200
0.302	.16470	0.332	.24200
0.603	.15310	0.664	.23800
0.905	.13790	0.996	.20000
1.206	.11660	1.327	.16730
1.508	.08929	1.659	.12580
1.809	.05843	1.991	.08412
2.111	.02877	2.323	.04265
2.412	.00900	2.655	.01276
2.714	.00144	2.987	.00162
3.015	.00009	3.319	.00006
3.317	.00000	3.650	.00000

P1 = .60

$\bar{F} = 3$

$\bar{F} = 4$

$\bar{r}$	$\bar{p}$	$\bar{r}$	$\bar{p}$
0.000	.23870	0.000	.27230
0.379	.23870	0.418	.27230
0.759	.22160	0.836	.25280
1.140	.20090	1.254	.22970
1.520	.17150	1.672	.19650
1.899	.13200	2.091	.15090
2.279	.08380	2.509	.09325
2.659	.03514	2.927	.03470
3.039	.00631	3.345	.00414
3.419	.00028	3.763	.00007
3.799	.00000	4.181	.00000

$\bar{F} = 5$

$\bar{F} = 6$

$\bar{r}$	$\bar{p}$	$\bar{r}$	$\bar{p}$
0.000	.28120	0.000	.37270
0.450	.28120	0.479	.37270
0.901	.25950	0.957	.35000
1.351	.23340	1.436	.29740
1.802	.19570	1.914	.23730
2.252	.14280	2.393	.17740
2.702	.07633	2.872	.10300
3.153	.01889	3.350	.02892
3.603	.00087	3.829	.00129
4.054	.00000	4.307	.00000

TABLE I

EXPERIMENTAL DATA

Stainless Steel (303)

Specimen Pair No. 1

$k = 10.0 \text{ BTU/HR.FT.}^{\circ}\text{F}$

<u>Specimen 1.1</u>	<u>Specimen 1.2</u>	<u>Combined Values</u>
$\sigma_1 = 81 \mu''$	$\sigma_2 = 69 \mu''$	$\sigma = 106 \mu''$
$R_1 = 10.4''$	$R_2 = 8.4''$	$R_1 = 4.65''$
$\text{Tan}_1\theta = .0512$	$\text{Tan}_2\theta = .0378$	$\text{Tan}\theta = .0635$

<u>F(Applied Load in Lbs.)</u>	<u><math>h(\text{BTU/HR.FT}^2\text{ }^{\circ}\text{F})</math></u>
165	10.7
265	12.5
365	13.9
765	20.0
1165	26.0
2165	32.8
3165	41.0
5165	54.7
7165	62.5
9765	85.7

TABLE II  
EXPERIMENTAL DATA

Stainless Steel (303)

Specimen Pair No. 2

$k = 10.0 \text{ BTU/HR.FT}^{\circ}\text{F}$

<u>Specimen 2.1</u>	<u>Specimen 2.2</u>	<u>Combined Values</u>
$\sigma_1 = 69 \mu''$	$\sigma_2 = 0 \mu''$	$\sigma = 69 \mu''$
$R_1 = 250''$	$R_2 = 156''$	$R_1 = 96''$
$\text{Tan}_1\theta = .068$	$\text{Tan}_2\theta = 0$	$\text{Tan}\theta = .068$

<u>F(Lbs.)</u>	<u><math>h(\text{BTU/HR.FT}^2\text{o}_F)</math></u>
165	49
265	71
365	88
565	101
765	124
1165	208

FIGURES

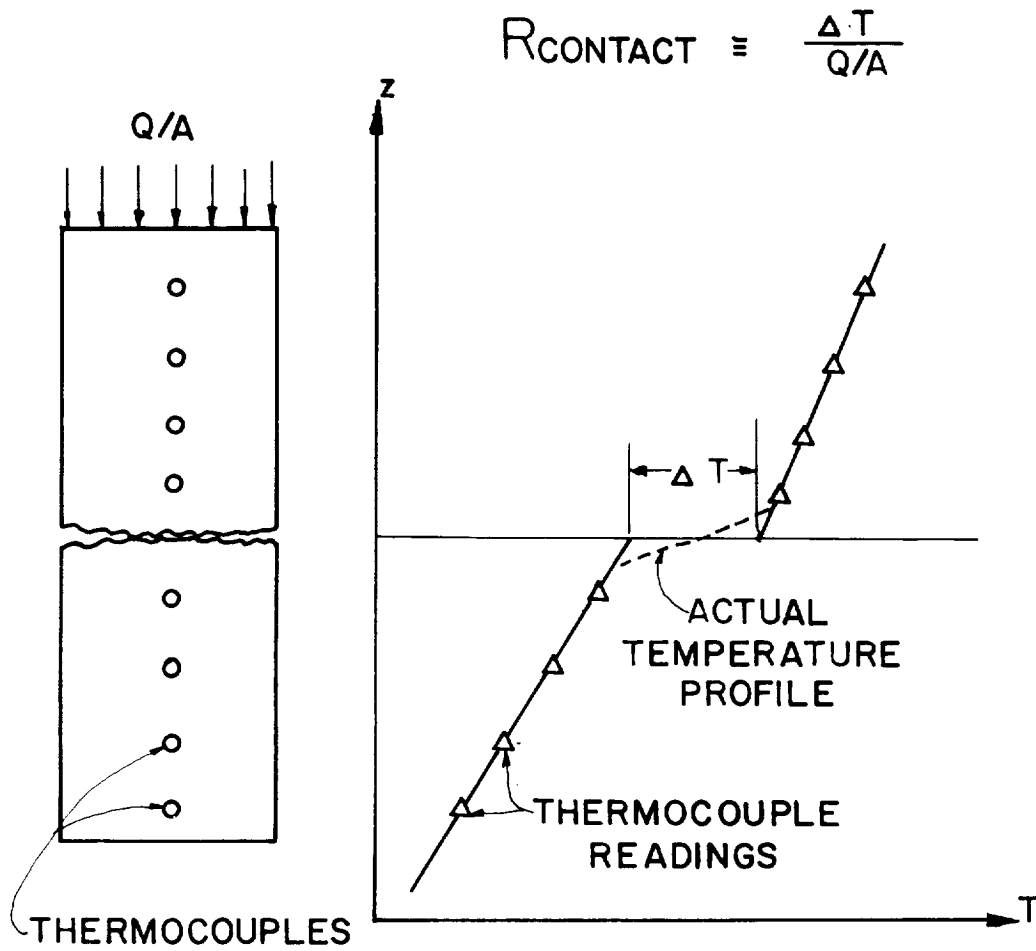


**FIG. 1 DEFINITION OF CONTACT RESISTANCE**



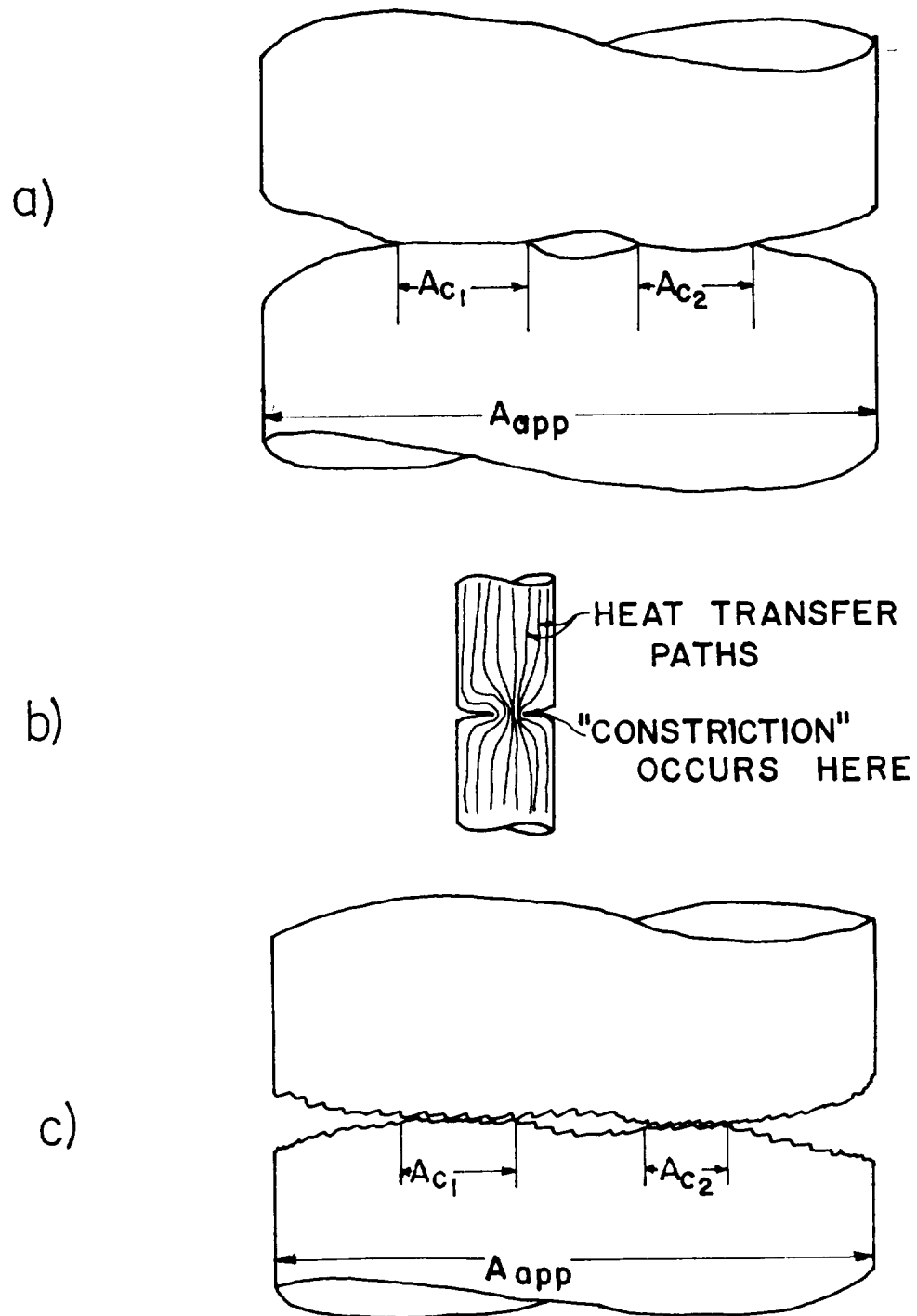
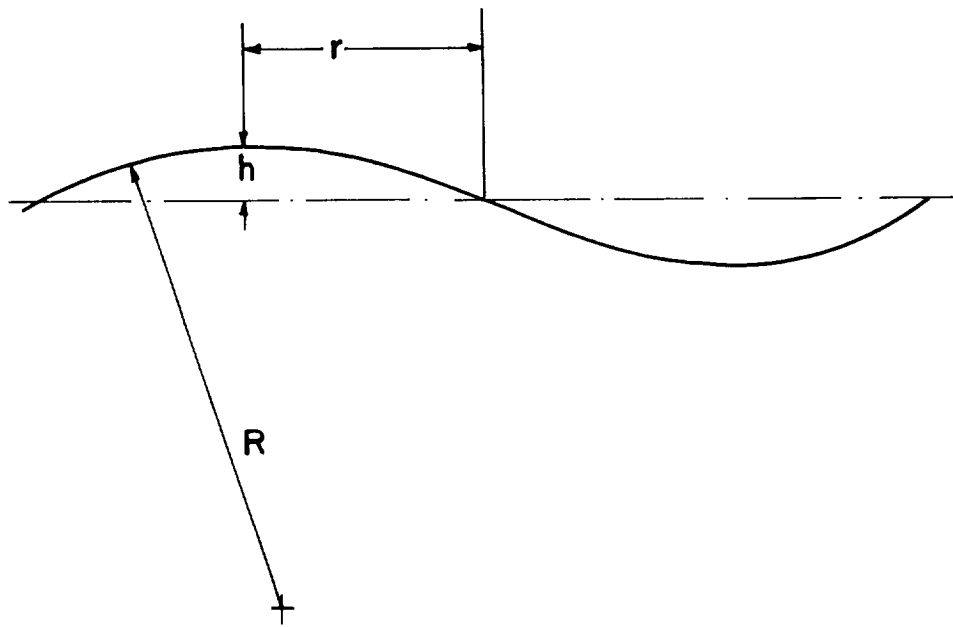


FIG. 2 SURFACE CONTACTS



**FIG. 3 SURFACE WAVINESS**

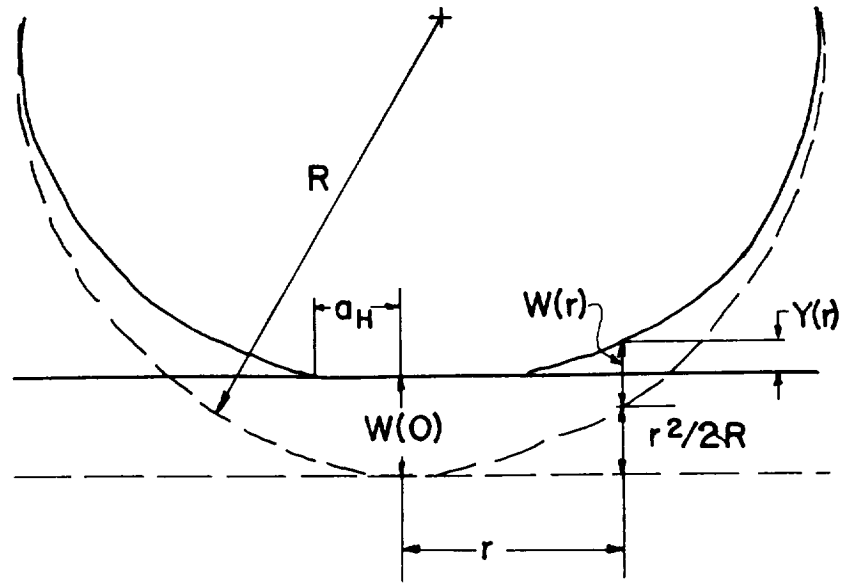


FIG. 4a SMOOTH SPHERE PRESSED AGAINST RIGID PLANE

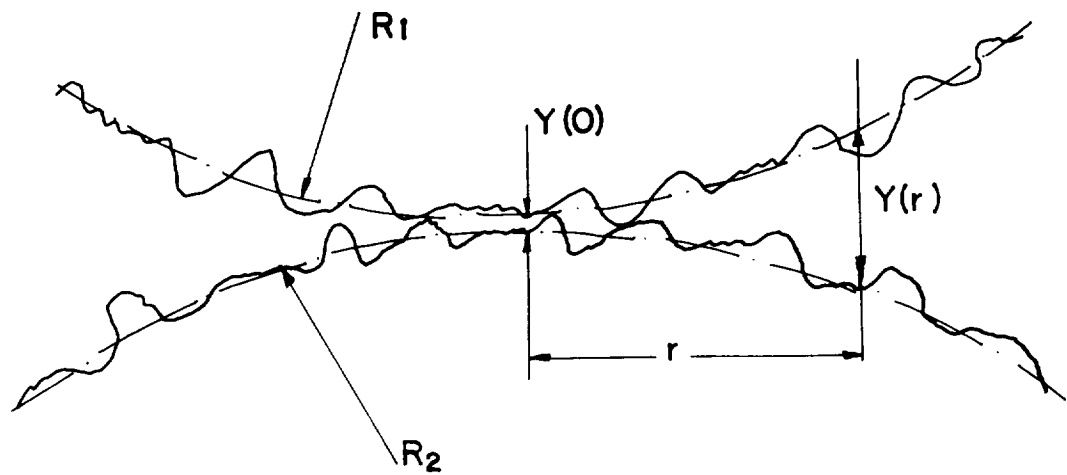


FIG. 4b TWO ROUGH SURFACES PRESSED TOGETHER

$$w(r) = \frac{1-\nu^2}{\pi E} \iint \frac{p}{\rho} dA$$

POINT (A) IS A POINT WHERE  $w(r)$  IS TO BE COMPUTED

POINT (B) IS THE ORIGIN OF A CIRCULAR COORDINATE SYSTEM

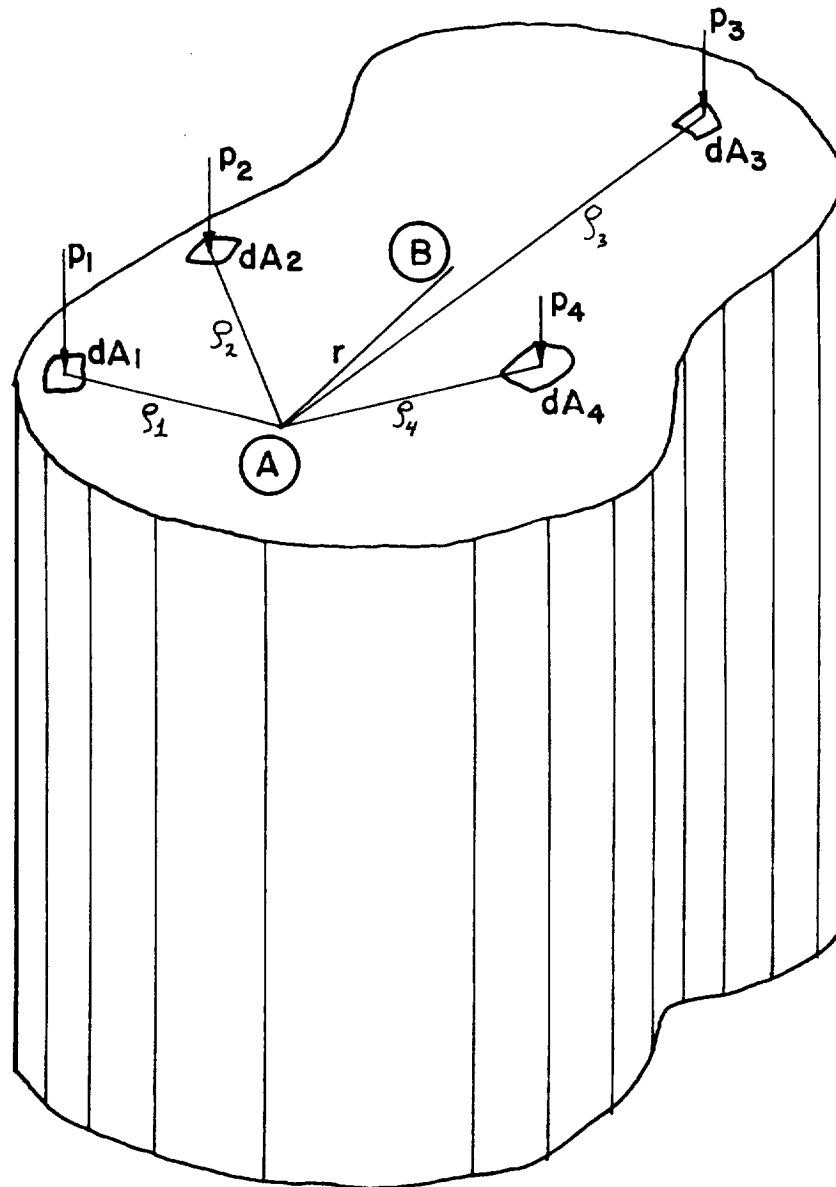


FIG. 5 TYPICAL CONTACT AREA

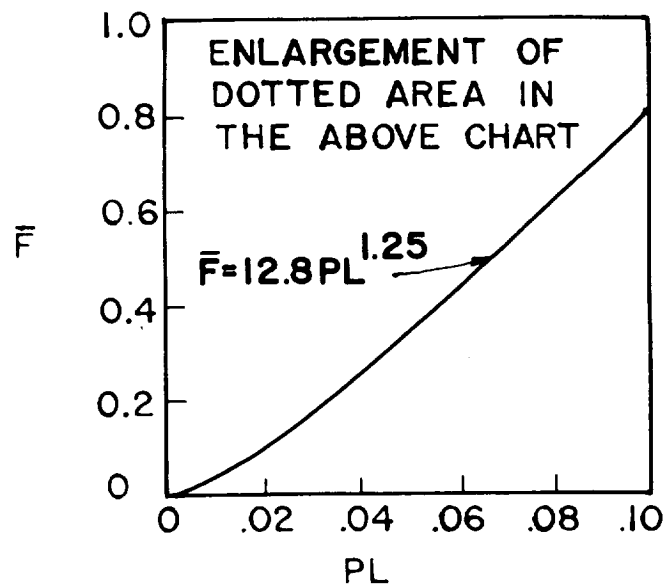
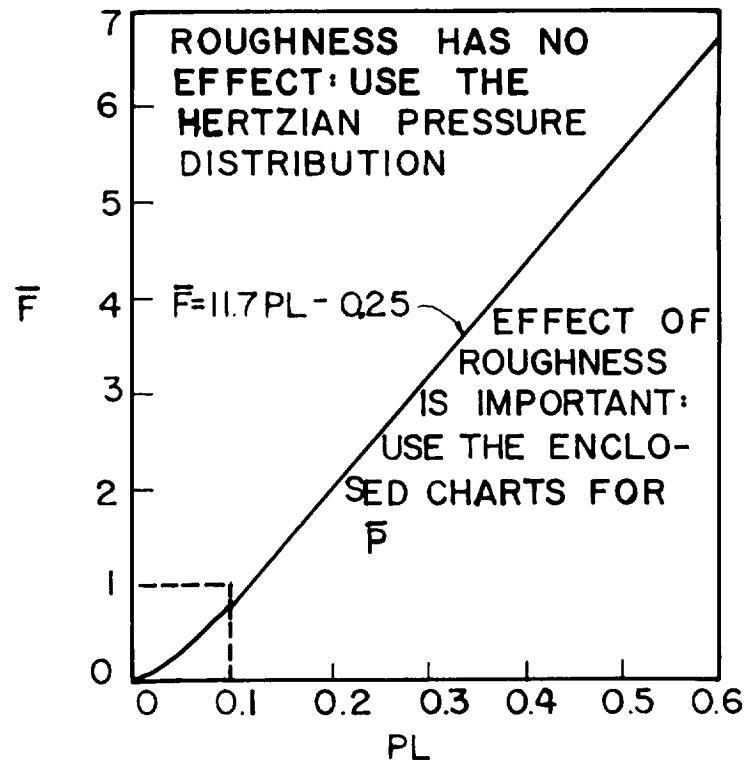


FIG. 6 REGION WHERE ROUGHNESS IS SIGNIFICANT

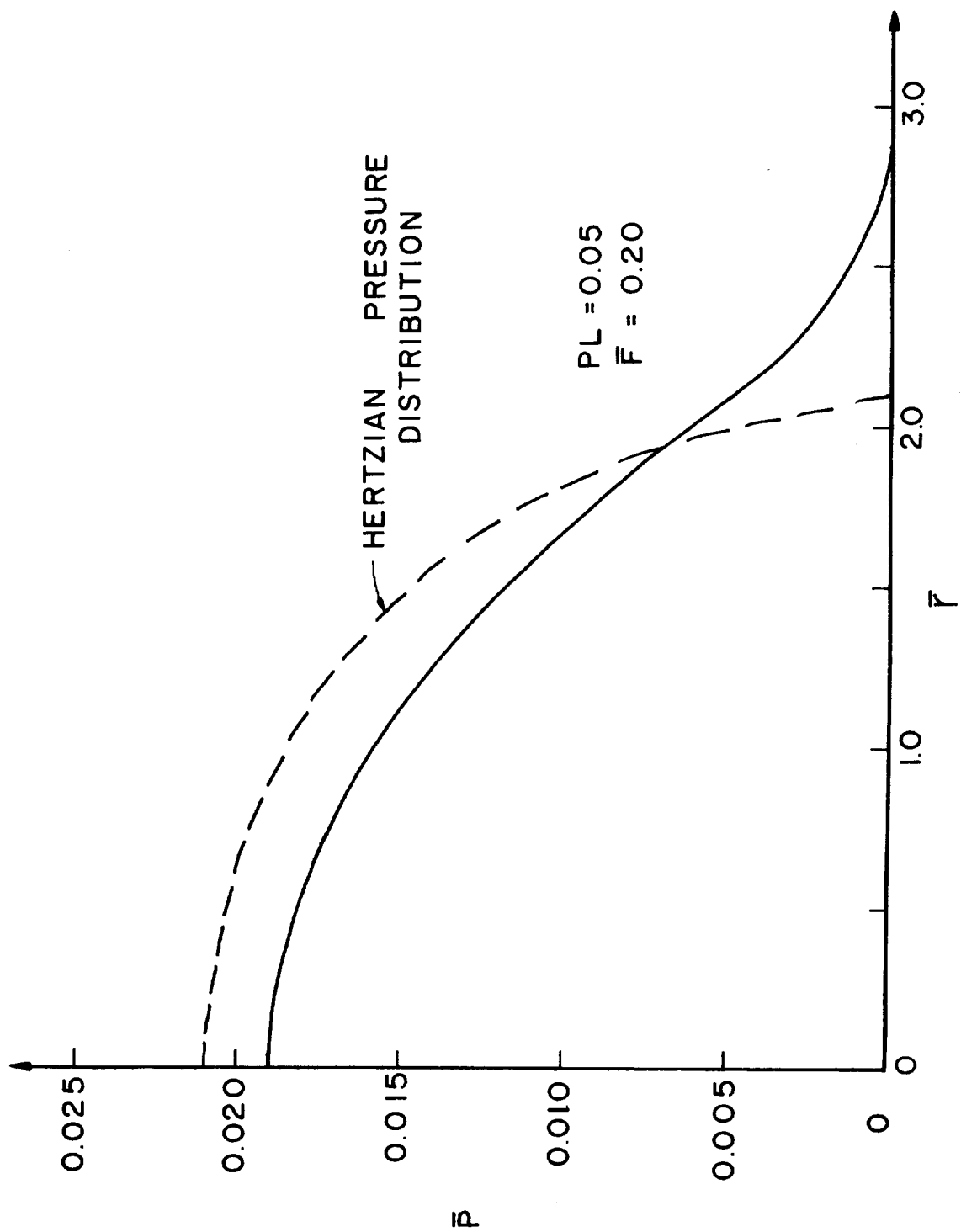


FIG. 7

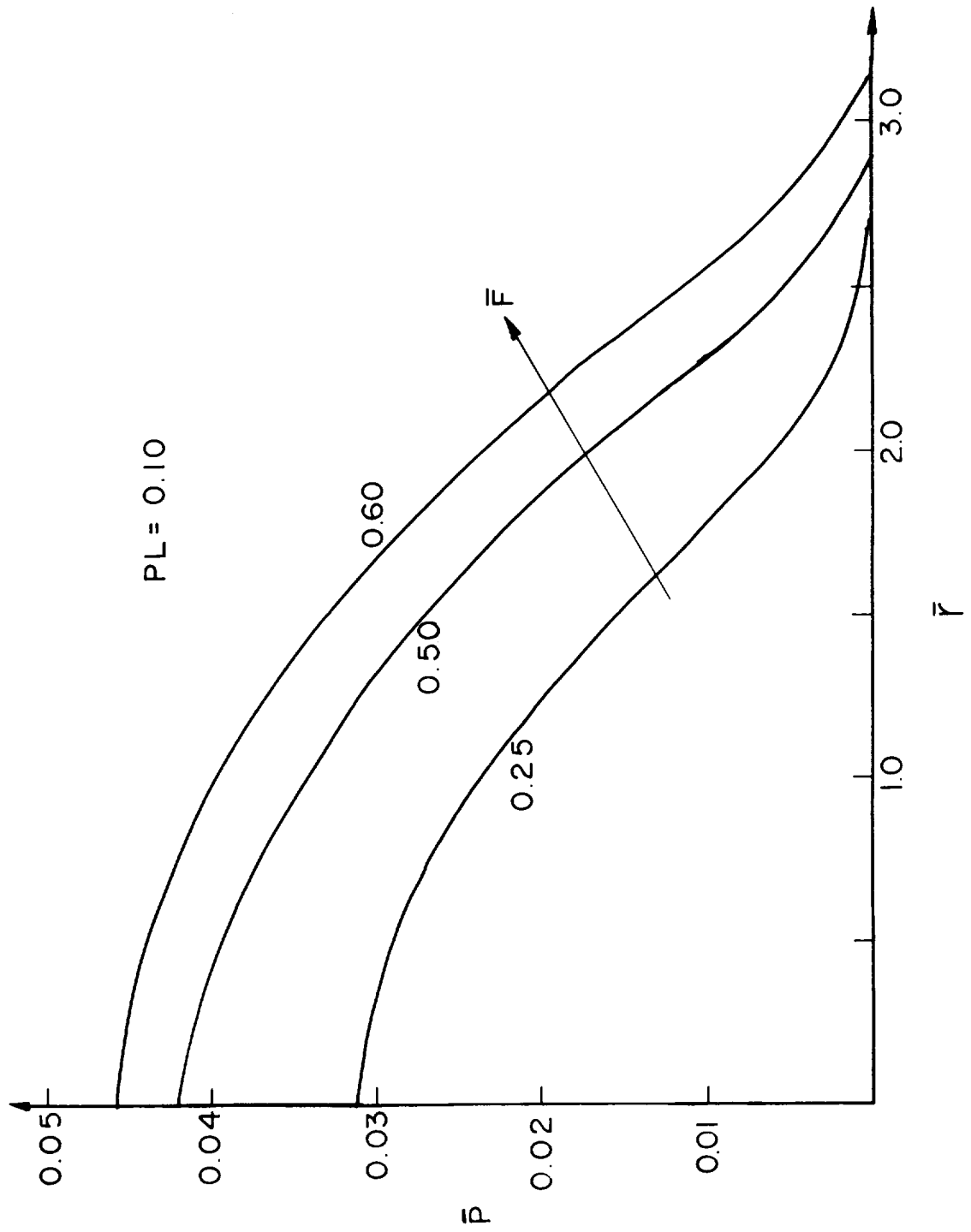


FIG. 8

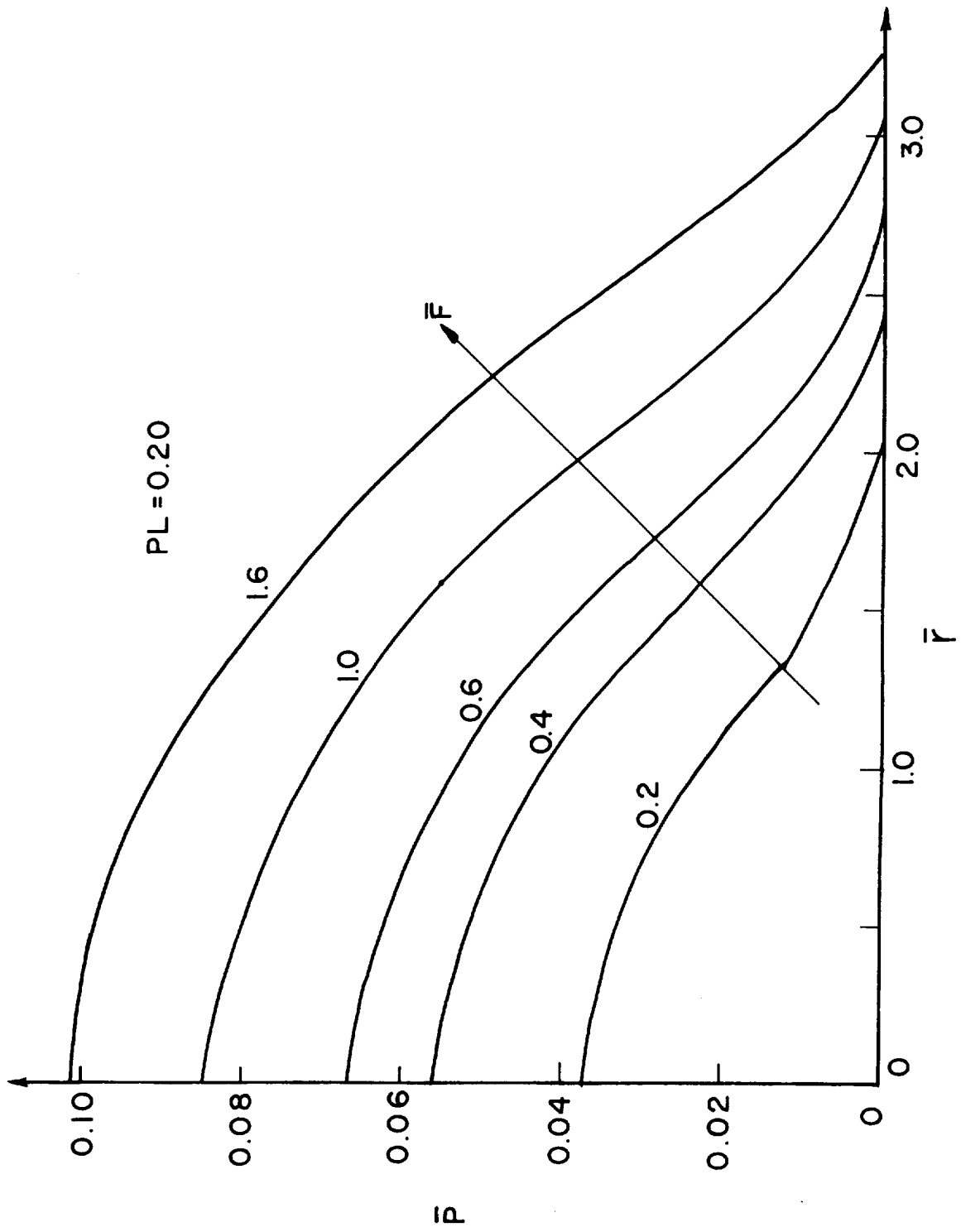


FIG. 9



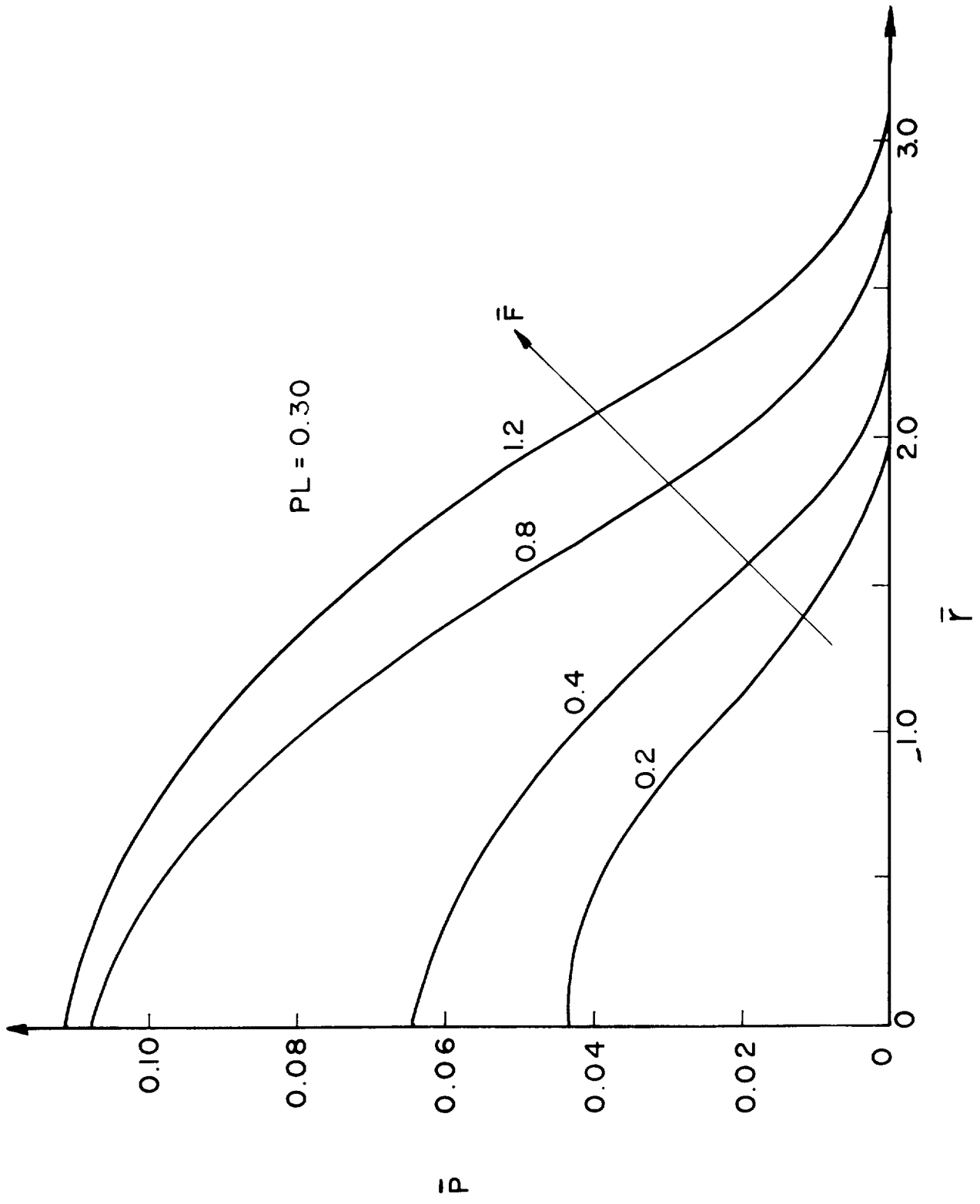


FIG. 10

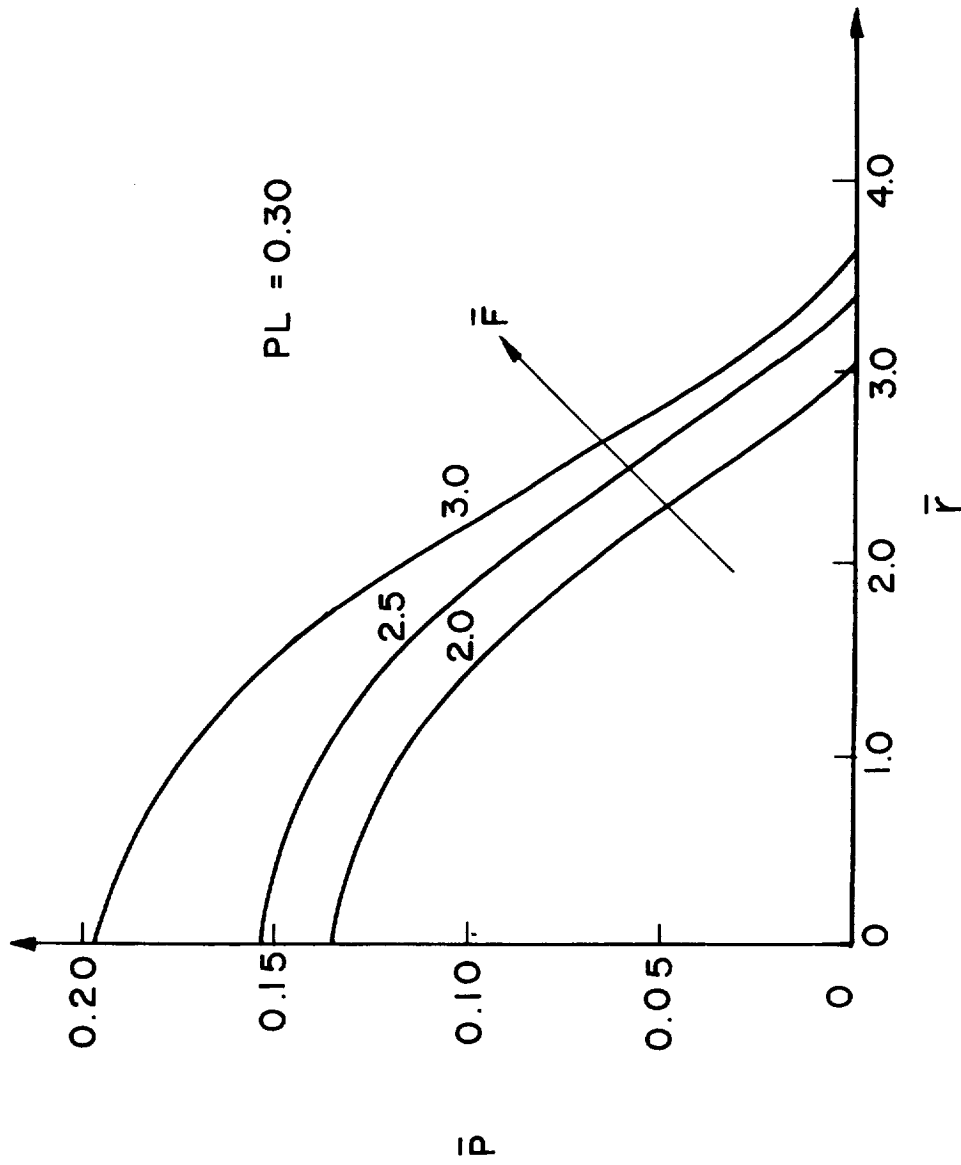


FIG. II

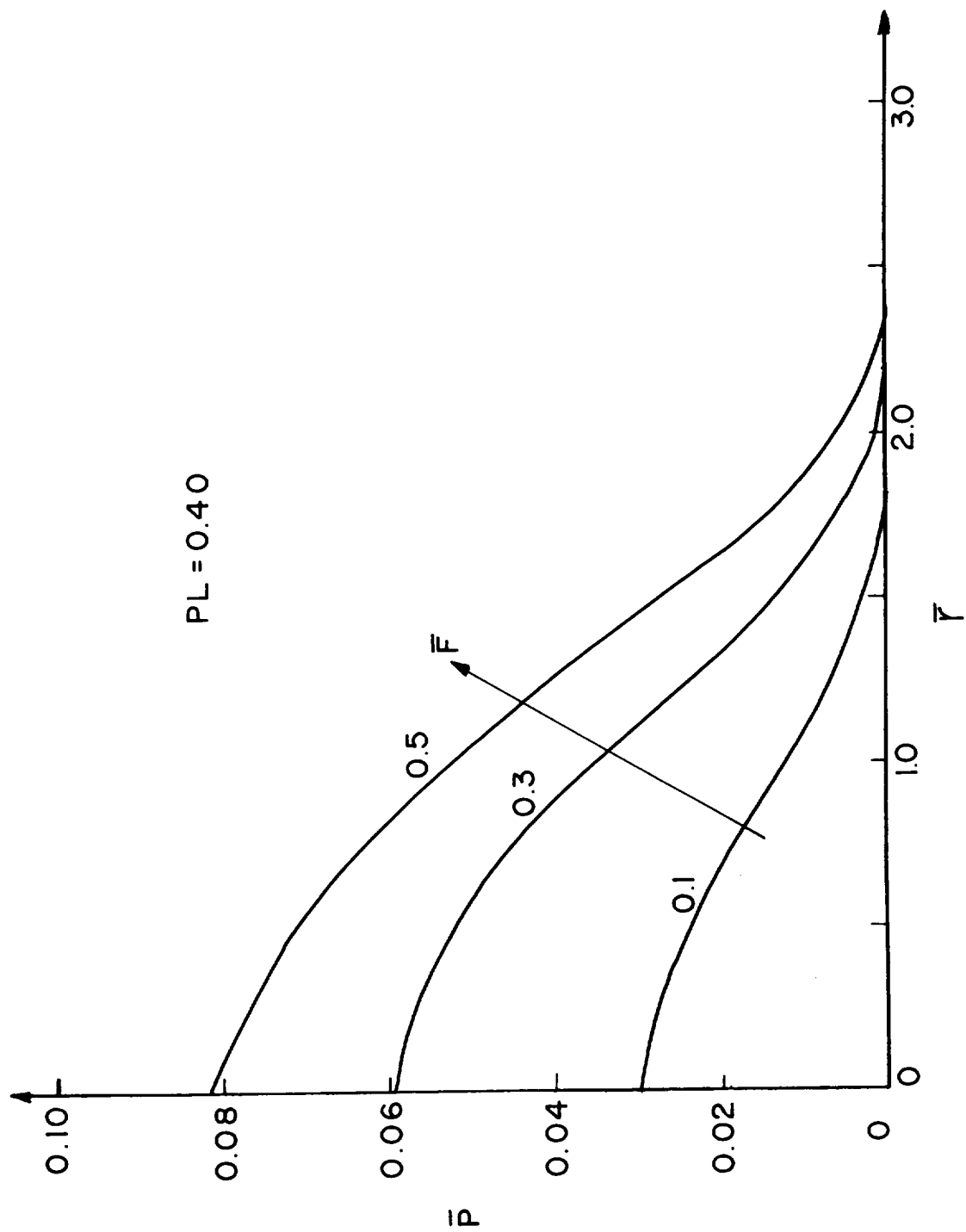


FIG. 12

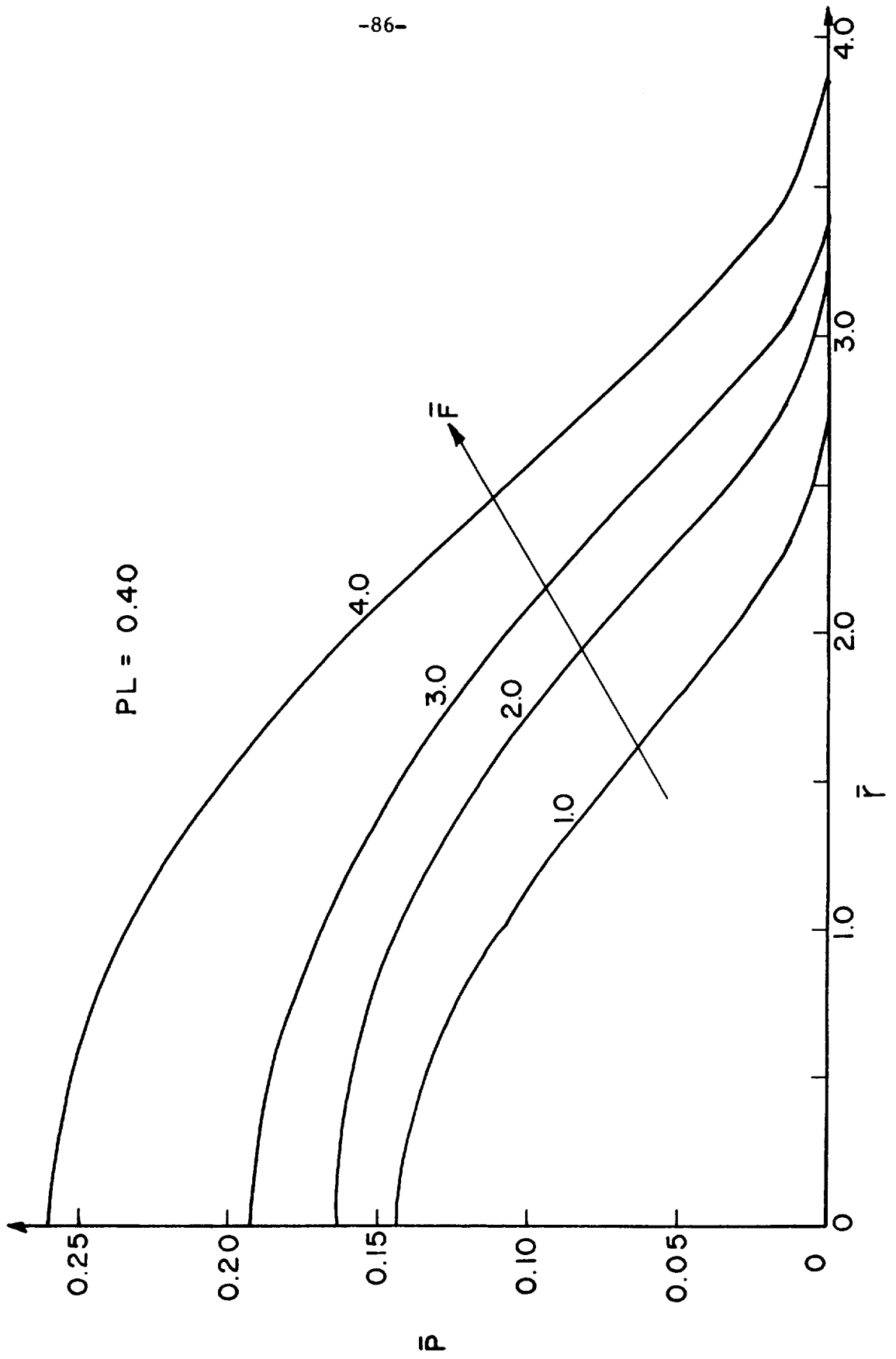


FIG. 13

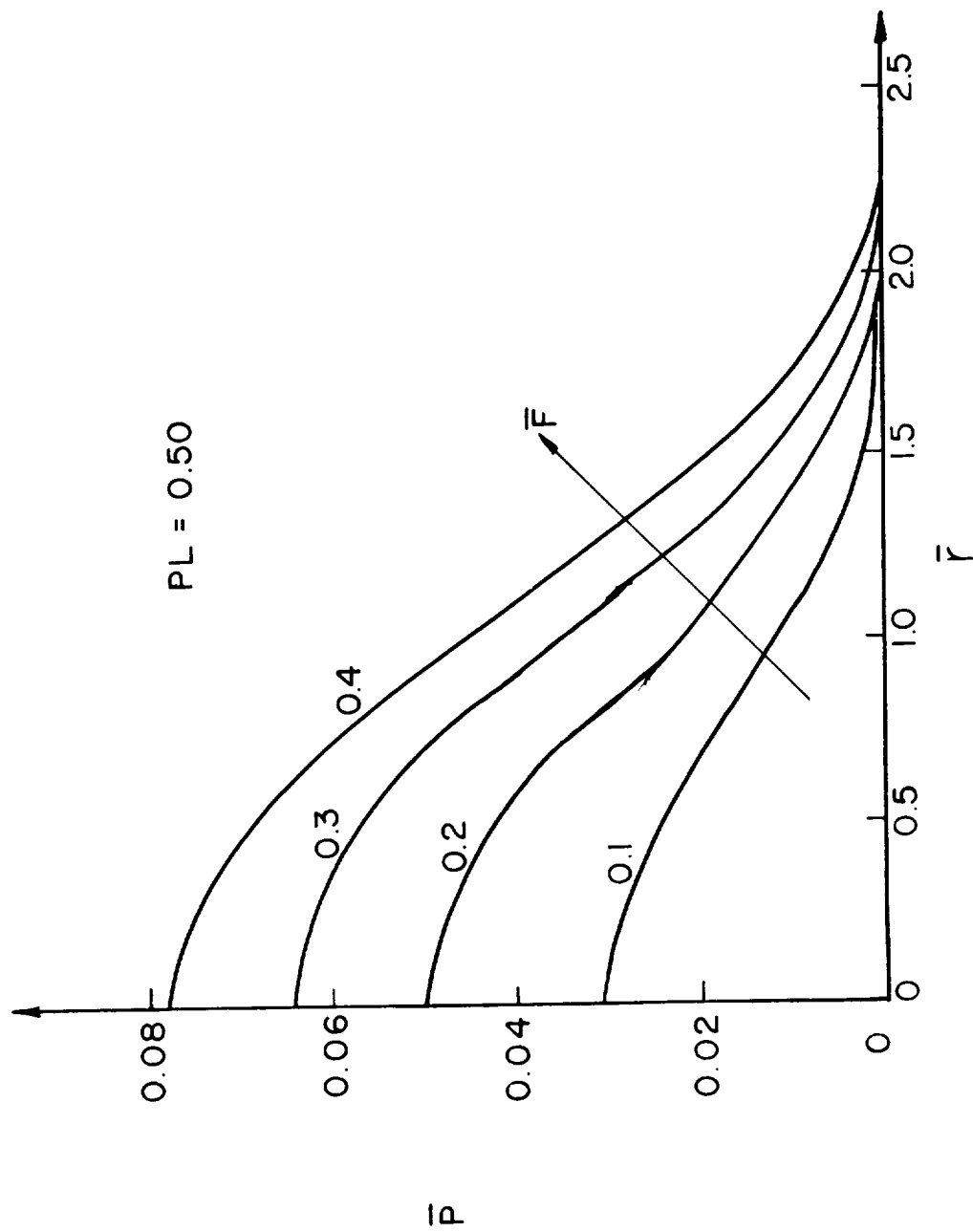


FIG. 14

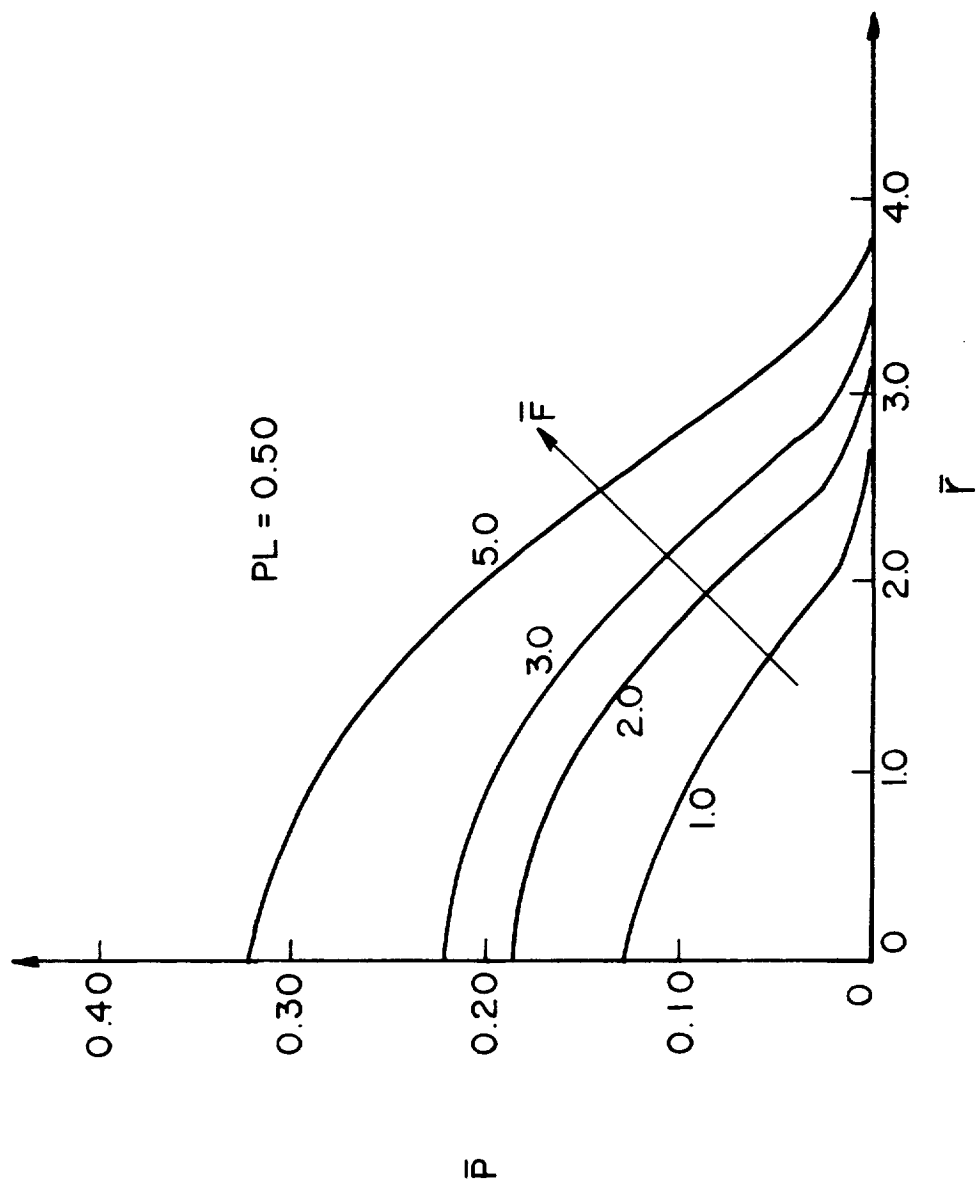


FIG. 15

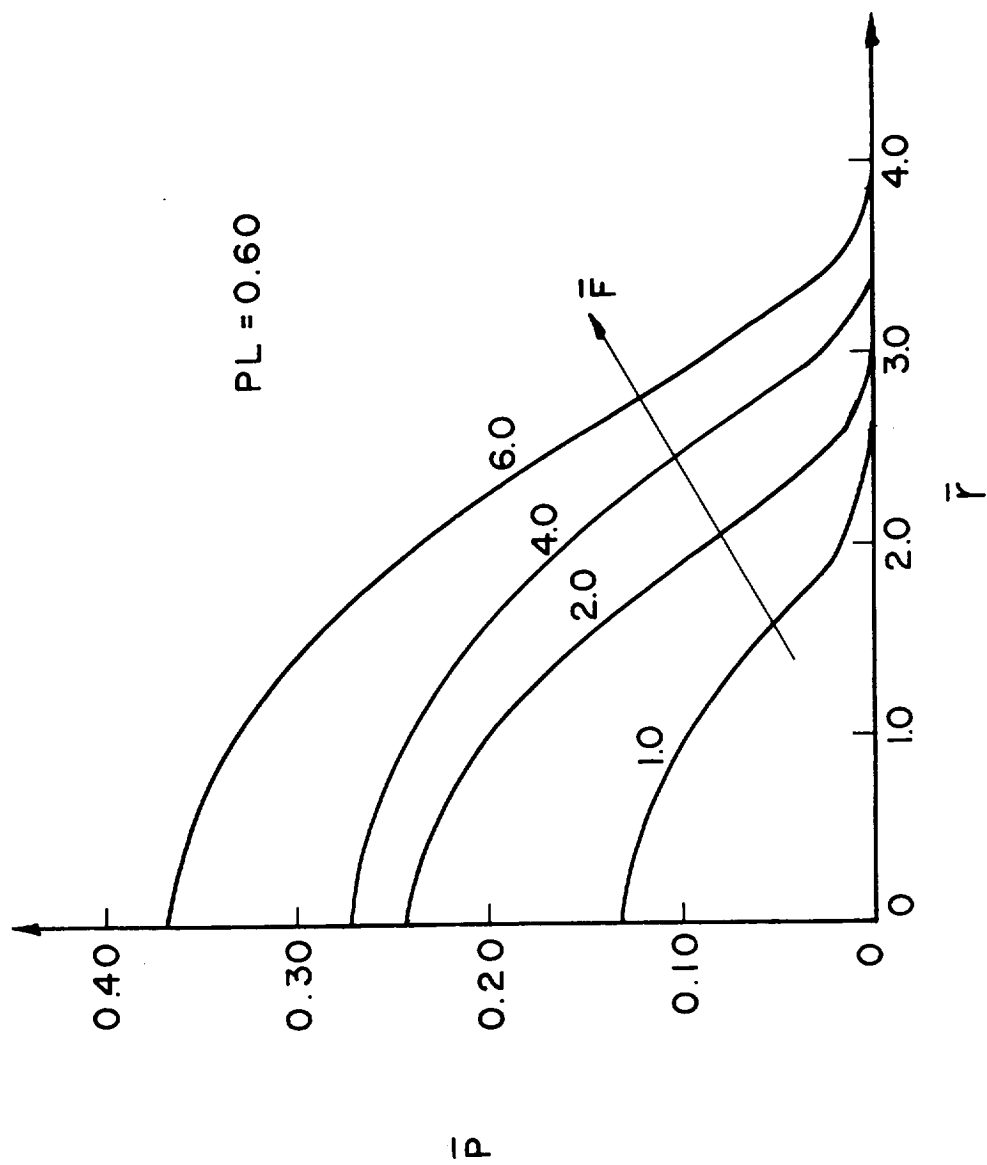
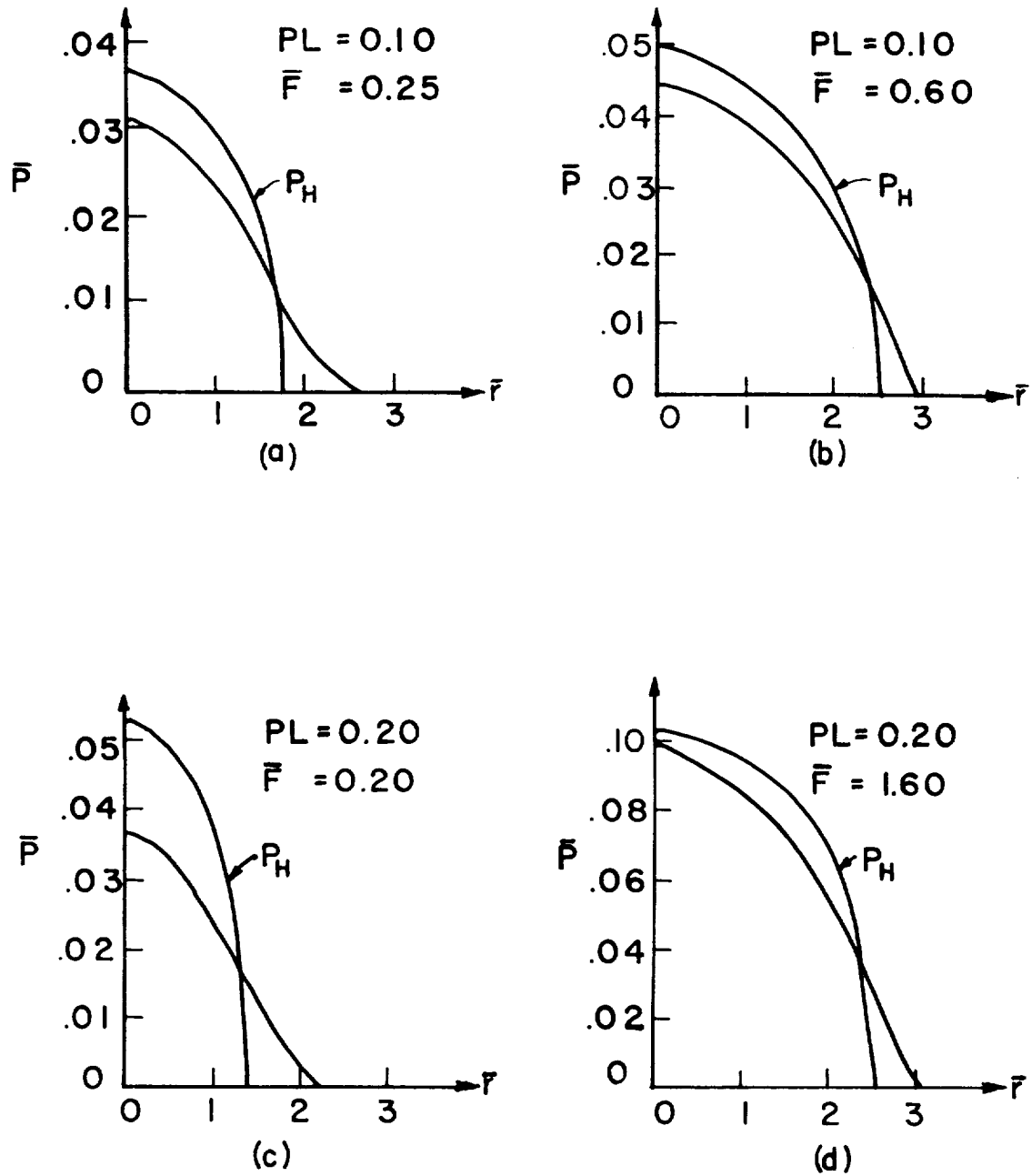
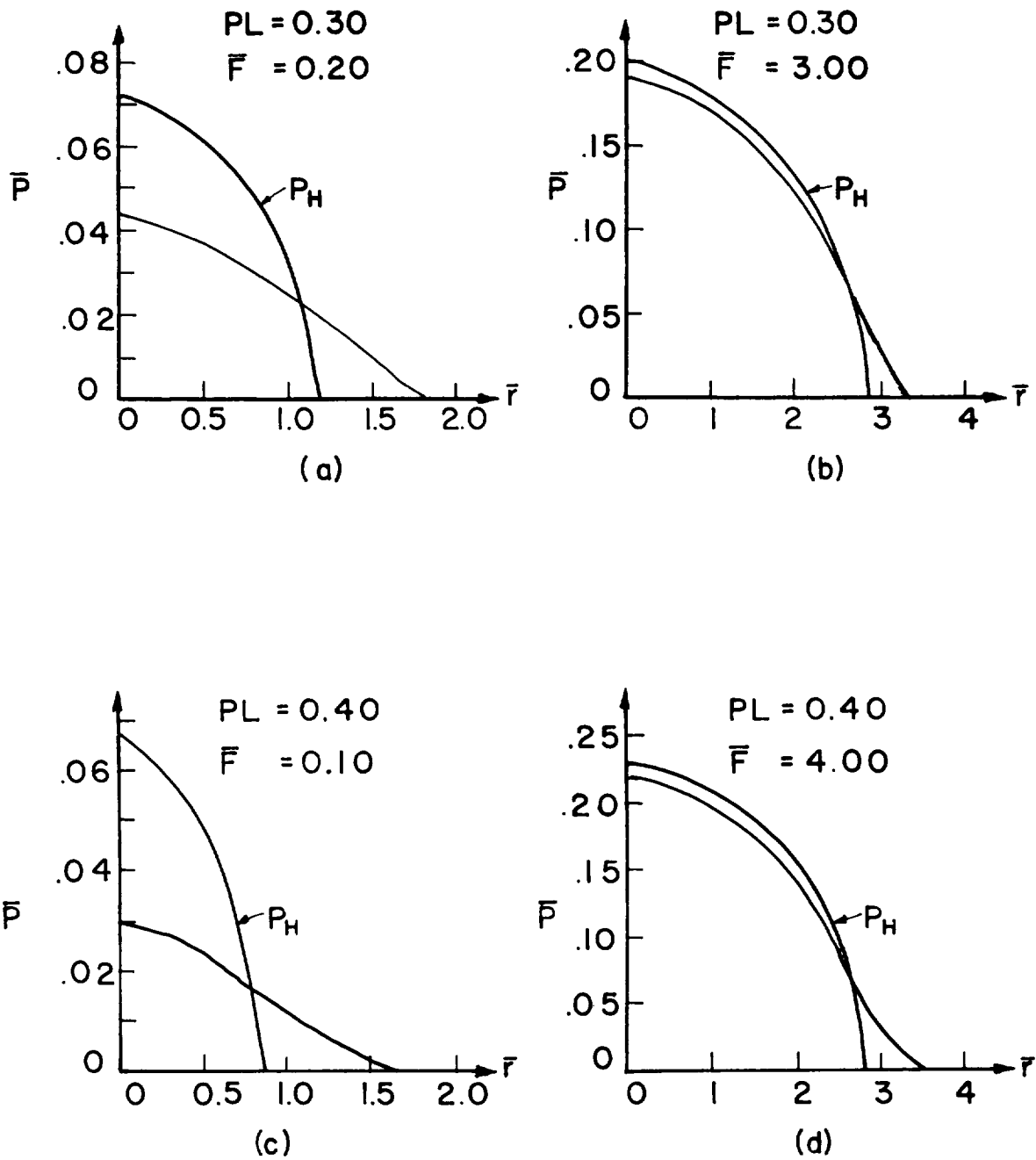


FIG. 16

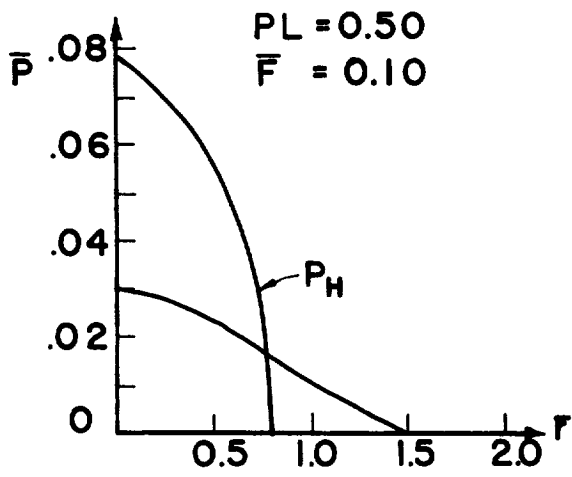


**FIG. 17 COMPARISON OF HERTZIAN ( $P_H$ ) AND ROUGH-SPHERE PRESSURE DISTRIBUTIONS**

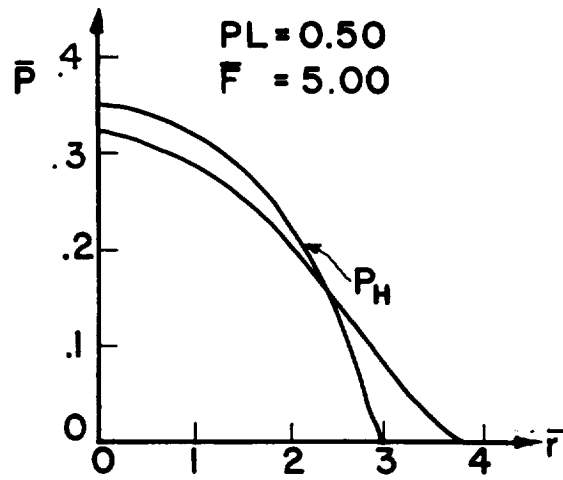




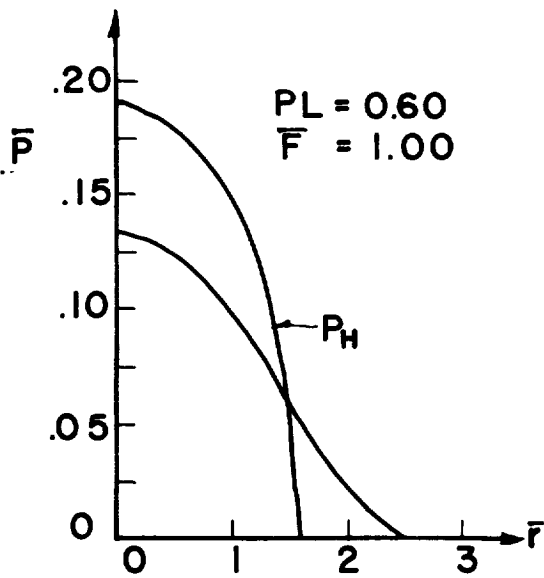
**FIG. 18 COMPARISON OF HERTZIAN ( $P_H$ ) AND ROUGH-SPHERE PRESSURE DISTRIBUTIONS**



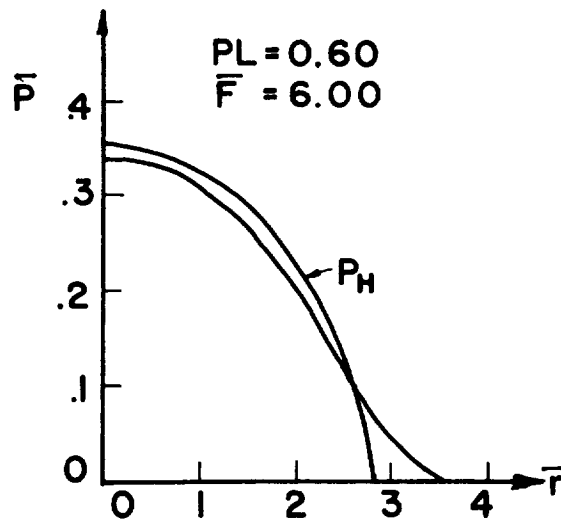
(a)



(b)



(c)



(d)

FIG. 19 COMPARISON OF HERTZIAN ( $P_H$ ) AND ROUGH-SPHERE PRESSURE DISTRIBUTIONS

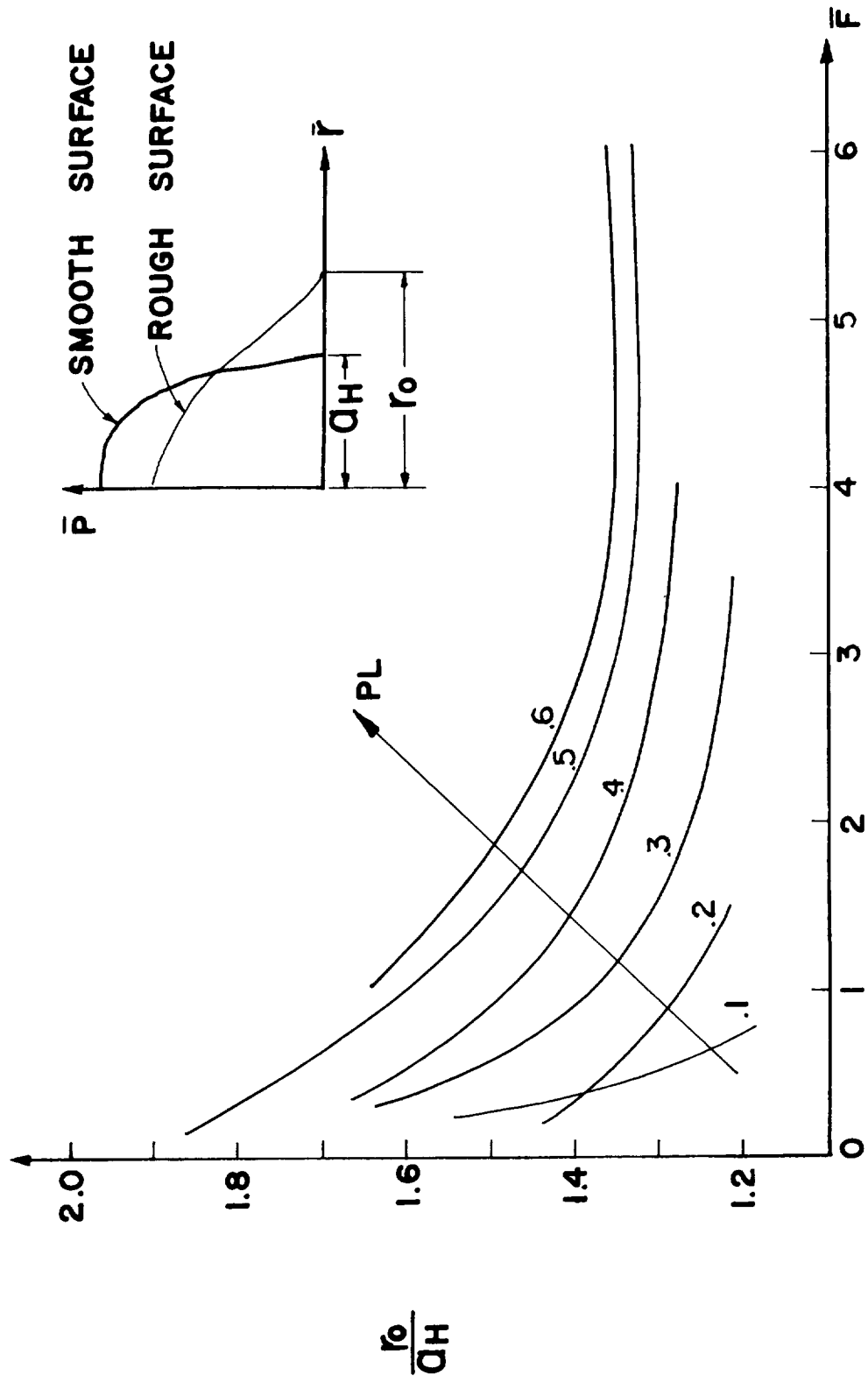


FIG. 20 RADIUS RATIO: SMOOTH VS. ROUGH SURFACES

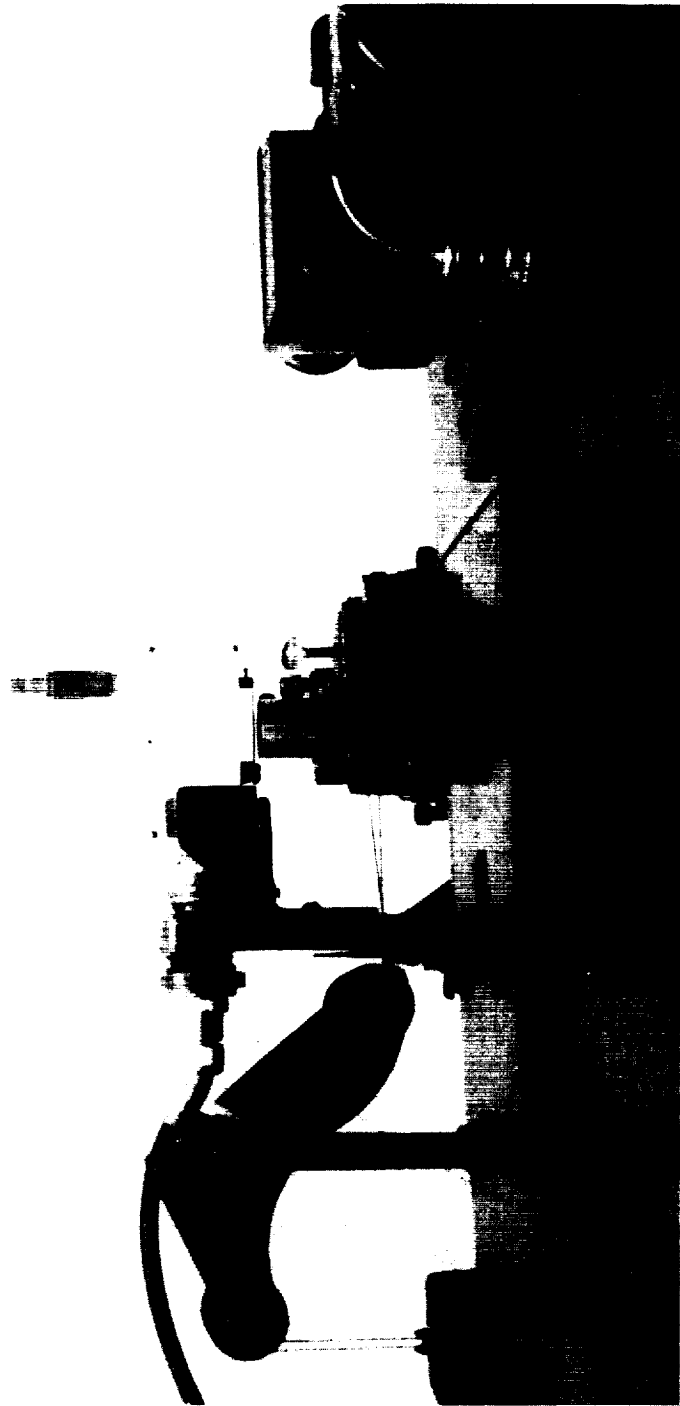


FIG. 21 SURFACE PROFILE MEASURING INSTRUMENT

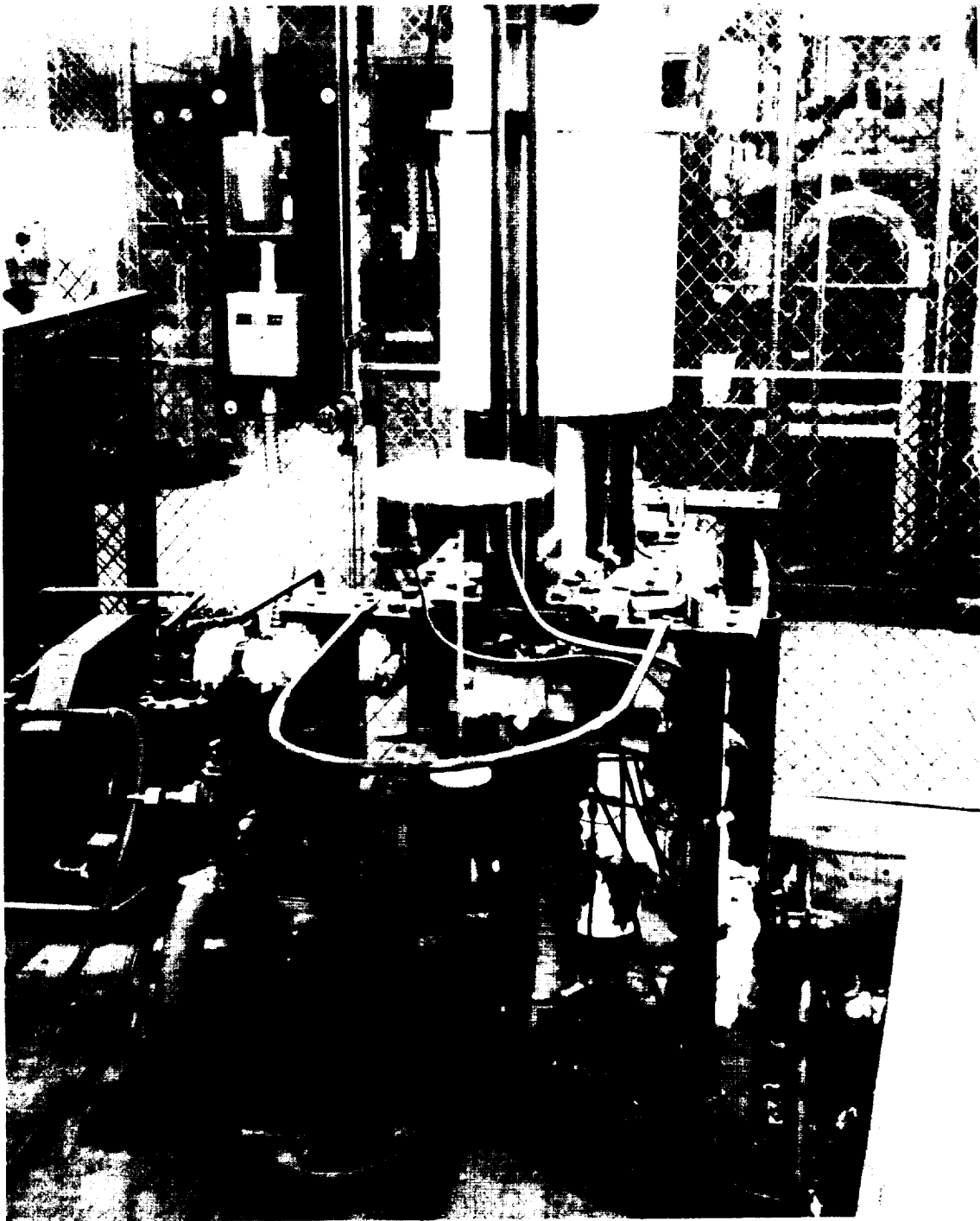


FIG. 22 CONTACT RESISTANCE APPARATUS

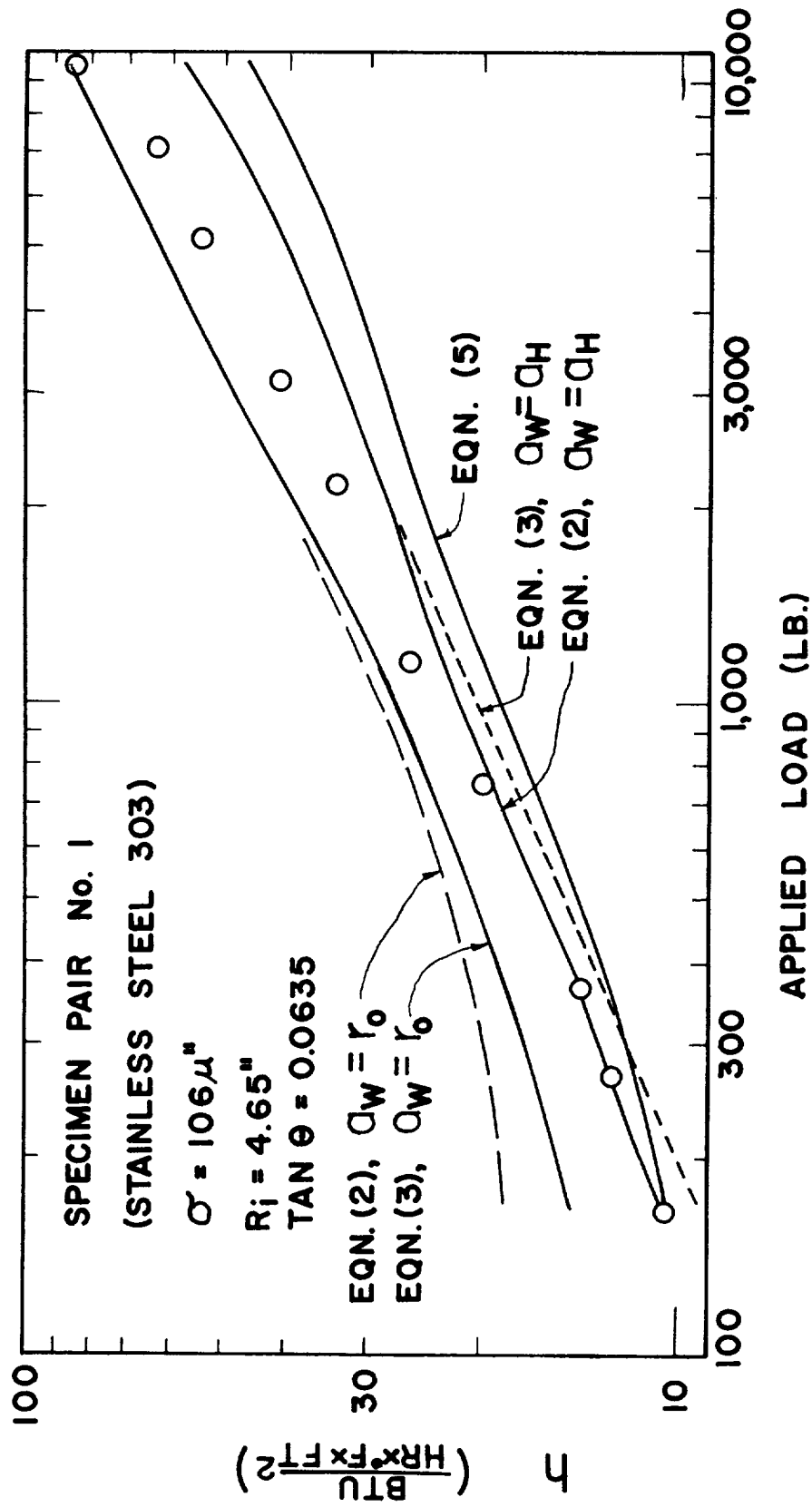


FIG. 23A. CONTACT CONDUCTANCE RESULTS

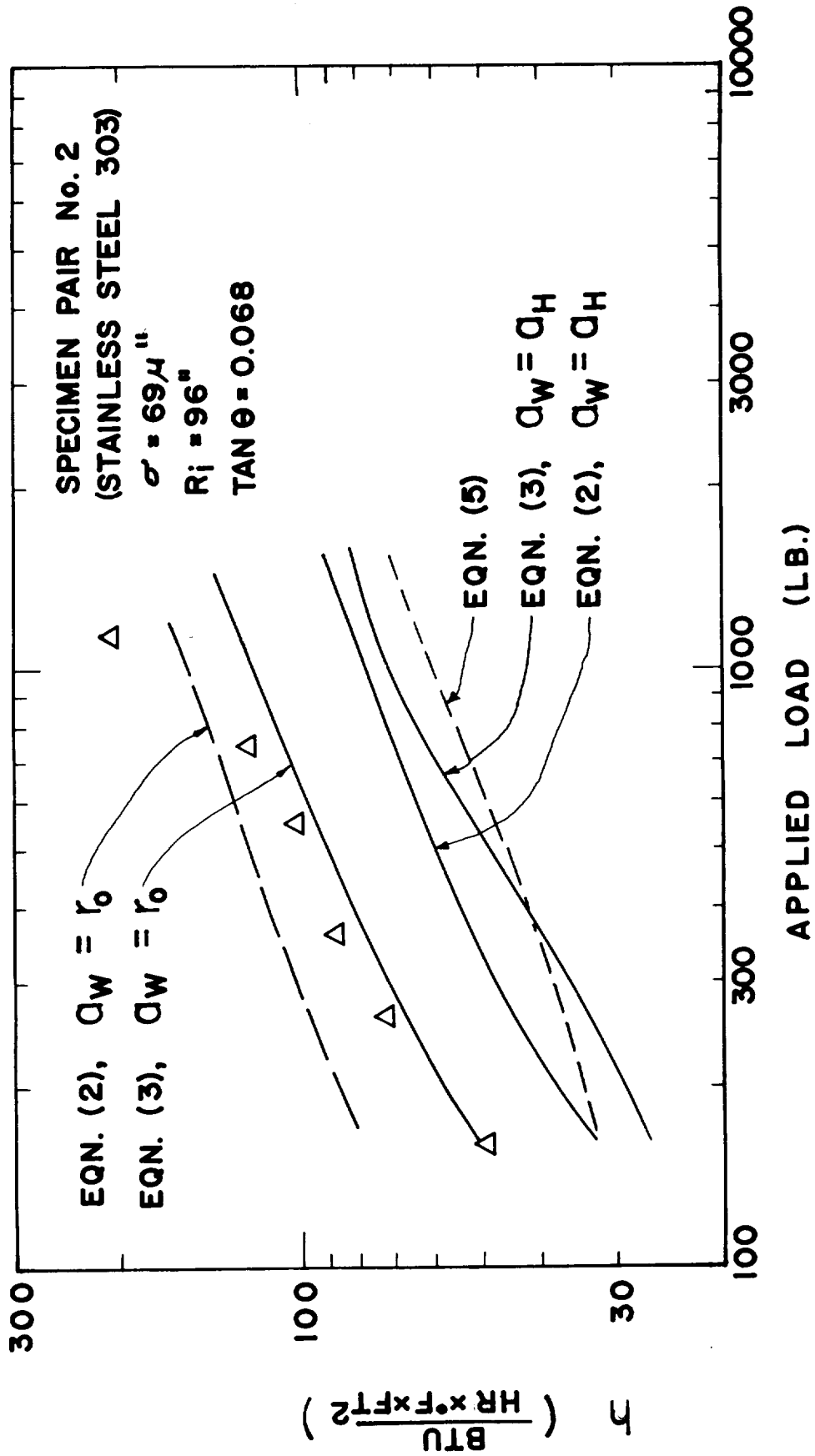


FIG. 23B. CONTACT CONDUCTANCE RESULTS

$T_0$  = AMBIENT TEMPERATURE

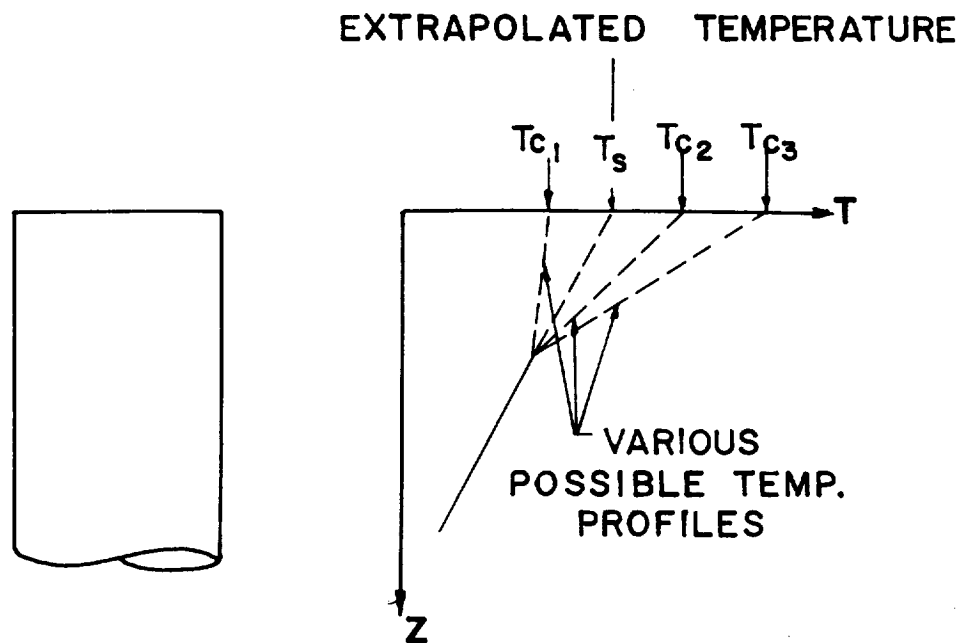
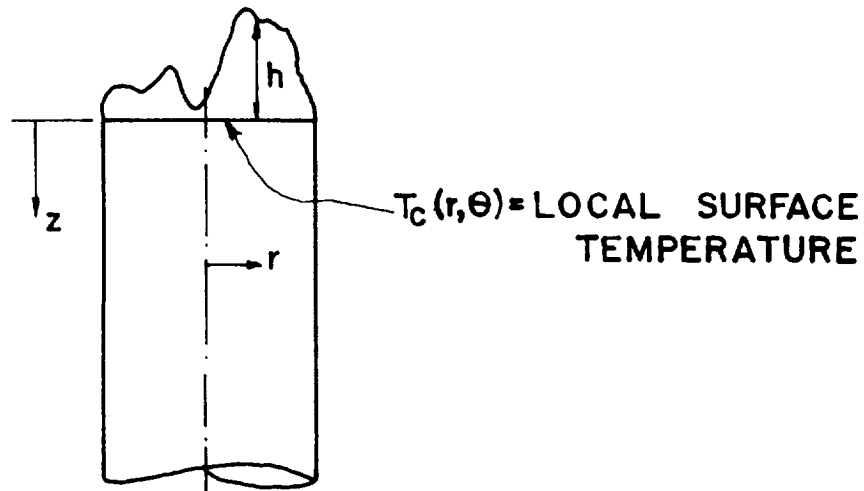
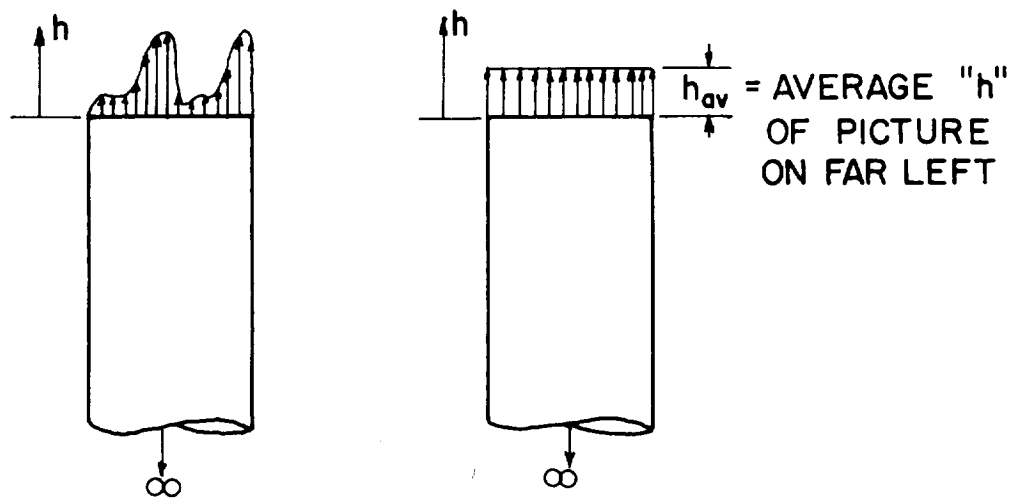
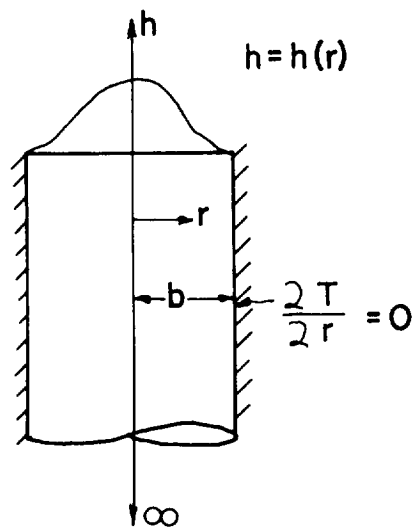


FIG. 24 NON - UNIFORM HEAT TRANSFER COEFFICIENT





(a)



(b)

FIG. 25 NON - UNIFORM HEAT TRANSFER COEFFICIENT

